A STUDY OF ABSORPTION AND REDDENING USING ABSOLUTE MAGNITUDES AND COLORS OF GALAXIES

Thesis by

Bruce Alrick Peterson

In Partial Fulfillment of the Requirements

For the Degree of

Doctor of Philosophy

California Institute of Technology

Pasadena, California

1969

(Submitted October 21, 1968)

To my parents

ACKNOWLEDGEMENTS

It is a pleasure for me to express my gratitude and esteem to Maarten Schmidt who suggested this project and guided me to its present conclusion.

I wish to express my appreciation to Allan Sandage for our discussions of philosophy and science, and for instructing me on the operation of the 100" Newtonian photometer.

My thanks to James Gunn, John Bahcall and John Faulkner for the delight and inspiration that I have gained from working with them.

To Armin Deutsch, who advised my first research project in observational astronomy, go my grateful thanks.

It has been a privilege and a pleasure for me to discourse and confer with Chip Arp, Willy Fowler, Bob Kraft, Bev Oke and Wall Sargent in the course of my studies.

I am indebted to Ben, Gene, Al, Ray, Henry, Gary and all the others on Mt. Wilson and Mt. Palomar who gave of their time at all hours of the day and night in order that the observations could proceed safely and efficiently, and who made a home for me while I was there.

My special thanks go to Ed Dennison and the staff of the Astro Electronics Laboratory for their part in making this project possible.

To Fritz Bartlett go my thanks for assistance and advice in dealing with the IBM 7090/94.

I gratefully acknowledge the financial support granted me by the National Areonautics and Space Administration Traineeship and by the subsequent Graduate Research and Teaching Assistantships. It has been a privilege to use the facilities of the Carnegie Institution of Washington and the California Institute of Technology in Pasadena and on Mt. Wilson and Mt. Palomar.

ABSTRACT

For the brightest galaxy in each of 48 nearby clusters and 7 groups of galaxies, photoelectric measurements of V and V-r magnitudes have been made. Redshifts have been measured for those 39 clusters and 3 groups which did not have previously published redshifts. Absolute magnitudes and colors were calculated for each cluster, and the cscb dependence of the absolute magnitudes and colors was attributed to galactic absorption.

After correcting for selection effects, the ratio of total to selective absorption was found to be $A_V/E_{V-r}=3.9$ which is consistent with $A_V/E_{B-V}=3.0$. The values found for the color-excess and absorption at the galactic pole are $E_{V-r}=0.016$ and $A_V=0.06$. This value for the color-excess is in ageement with $E_{B-V}=0.03$ found by Sturch for the RR Lyrae stars.

TABLE OF CONTENTS

I. INTRODUCTION

The most commonly used value for the amount of absorption suffered by an object at the galactic pole is $A_{pg}=0.25$ which was determined by Hubble (1934) from galaxy counts. A study by Holmberg (1958) of the surface brightness of spiral galaxies also yielded a similar value, $A_{pg}=0.26$.

However, a re-analysis of Hubble's data with a correction for redshift by Oort (1938) and by Shane and Wirtanen (1967) lead to values of 0.31 and 0.46, respectively, for the photographic absorption at the pole. Shane and Wirtanen (1967) have also used their recently completed galaxy counts to determine the absorption. They found $A_{pg}=0.51$.

Neckel (1965) pointed out that Holmberg's determination was subject to a systematic error in that the isophote to which the surface brightness had been measured depended upon the amount of absorption present. After correcting for this effect, Neckel found that Holmberg's data gave $A_{pg}=0.46$.

Using Whitford's (1958) determination of absorption as a function of wavelength and $A_{pg}=0.5$, the expected color-excess at the galactic pole is $E_{B-V}=0.12$. However, this value for E_{B-V} is too large. Arp (1962) has pointed out that Holmberg's galaxy colors, and the integrated colors of globular clusters (Stebbins, 1933, and Kron and Mayall, 1960), yield $E_{B-V}=0.06$. Sandage (1964a, 1964b) has shown that the high latitude globular clusters have the same reddening as the field RR Lyrae stars, which are assumed to have zero

reddening. More recently, Sturch (1966) has used field RR Lyrae stars at high galactic latitudes to obtain $E_{B-V}=0.03$ with the assumption that they lie, for the most part, above the material producing the reddening. Taken together, the worksof Sandage and Sturch indicate $E_{B-V}=0.03$ (Sturch, 1967).

The ratio of total to selective absorption would have to be greater than 6 to reconcile the high values for the absorption with these low values for the reddening.

In order to provide an independent determination of the amount of absorption produced by the material in the galactic plane, as well as an independent determination of the ratio of total to selective absorption, I have examined the galactic latitude dependence of the colors and luminosities of the brightest galaxies in nearby clusters of galaxies.

The clusters were selected from Abell's (1958) catalogue on the basis of the photo-red magnitude which was given for the 10th brightest cluster galaxy. All clusters as bright as 15.0 were used, and for those below a galactic latitude of 30^{o}, all clusters as bright as 15.6 were used. In addition to the clusters, four groups of galaxies investigated by Humason, Mayall and Sandage (1956) and three groups of galaxies found from inspection of the National Geographic Society - Palomar Observatory Sky Survey prints were included in the study.

An area of approximately one square degree, centered

on the position of each cluster, was examined for the brightest galaxy, using the Sky Survey prints. Table 1 gives the Abell cluster number, 1950 equatorial coordinates, new galactic coordinates and NGC or IC number for the galaxy judged to be the brightest in each cluster. The seven groups of galaxies are included at the end of the table.

Photometric measurements of each galaxy were made in the V and r pass bands at effective wavelengths of λ5400 and λ6750, respectively. Redshifts were measured for all galaxies which did not have previously published redshifts. Absolute magnitudes and colors were then calculated for all of the program galaxies with the assumption that the redshifts are cosmological, and thus indicate the distance of the galaxies.

The systematic variation of the absolute magnitudes and colors with galactic latitude is attributed to galactic absorption.

Table 1

Equatorial and Galactic Coordinates of Brightest Galaxy in Cluster or Group

Cluster	RA 1950	DEC 1950	LONG	LAT	NGC or IC
76	00 36 50	06 27 45	117 35	-56 01	IC 1565
119	00 53 41	-01 32 10	125 41	-64 07	
147	01 05 34	01 54 59	131 25	-60 25	
151	01 06 22	-15 40 13	142 50	-77 36	IC 80
194	01 23 24	-01 36 09	142 10	-62 55	NGC 545
262	01 49 47	35 54 34	136 33	-25 05	NGC 708
278	01 54 19	32 01 06	138 45	-28 35	
347	02 22 16	41 36 18	141 06	-17 42	NGC 910
376	02 42 53	36 41 35	147 05	-20 32	
400	02 55 01	05 49 11	170 16	-44 56	
407	02 58 44	35 38 23	150 37	-19 56	
426	03 16 28	41 20 12	150 34	-13 16	NGC 1275
505	04 51 12	80 06 09	132 18	22 14	
539	05 13 56	06 23 05	195 43	-17 43	
548	05 46 37	-25 29 38	230 17	-24 26	
553	06 08 50	48 36 45	165 09	14 03	
568	07 04 20	35 08 39	182 13	18 16	
569	07 05 19	48 41 54	168 34	22 48	NGC 2329
576	07 17 23	55 51 30	161 23	26 16	
592	07 39 54	09 29 53	210 14	15 36	
634	08 11 38	58 28 18	159 04	33 47	
671	08 25 24	30 36 13	192 44	33 07	IC 2378
754	09 06 04	-09 25 11	239 11	24 42	
779	09 16 44	33 57 29	191 06	44 23	NGC 2832
993	10 19 22	-04 37 30	248 45	41 45	
1060	10 34 12	-27 14 36	269 33	26 29	NGC 3309
1139	10 55 33	01 52 52	251 21	52 45	
1185	11 07 55	29 02 20	202 48	67 43	NGC 3550
1213	11 13 29	29 39 50	201 10	68 56	
1228	11 18 38	34 37 56	186 53	69 23	IC 2738

Table 1 (contd.)

Cluster	RA 1950	DEC 1950	LONG	LAT	NGC or IC
1257	11 23 34	35 36 40	183 21	70 05	
1314	11 32 07	49 20 44	151 46	63 33	IC 712
1318	11 32 56	55 13 23	144 07	58 57	NGC 3737
1367	11 41 23	20 13 43	234 16	72 59	NGC 3842
1377	11 44 40	56 01 04	140 24	59 10	
1656	12 57 07	28 13 28	58 08	88 01	NGC 4874
1736	13 23 58	-26 52 33	312 32	35 05	
2052	15 14 12	07 11 54	9 24	50 08	
2147	15 59 56	16 06 32	28 54	44 32	
2151	16 02 51	17 51 11	31 32	44 33	NGC 6045
2152	16 03 08	16 33 45	29 53	44 00	
2162	16 10 31	29 36 11	49 19	46 01	NGC 6086
2197	16 28 01	40 54 47	64 40	43 31	NGC 6173
2199	16 26 49	39 39 03	62 55	43 43	NGC 6166
2319	19 19 33	43 50 51	75 41	13 31	
2634	23 35 55	26 45 21	103 29	-33 04	NGC 7720
2657	23 41 56	08 59 35	96 36	-50 09	
2666	23 48 21	26 52 15	106 42	-33 48	NGC 7768
03+3909	03 40 34	39 08 56	155 42	-12 21	
22+3552	22 21 52	35 52 08	92 21	-17 51	NCG 6049
01+3300	01 20 46	32 59 51	130 37	-29 08	NGC 507
01+3209	01 04 35	32 09 05	126 49	-30 20	NGC 383
01+0523	01 53 42	05 23 23	150 55	-53 41	NGC 741
04-0511	04 29 11	-05 11 20	200 25	-33 15	NGC 1600
22+3505	22 36 05	35 05 01	94 29	-20 04	

II. OBSERVATIONS

Photometric Measurements

The UBVr photometric system used for the observations is that of Sandage and Smith (1963). The U,B, and V filters have been chosen to reproduce the U,B, and V band passes of the UBV system of Johnson and Morgan (1953). The components of my filters, which differ slightly from those of Sandage and Smith, are given in Table 2.

TABLE 2

UBVr FILTER COMPONENTS

U	2.8mm Corning 9863 + 5mm of 40% saturated sol. at 0°C of Cu $SO_4 \cdot 5 H_2O$ in a liquid cell* with two quartz windows.
B	2.0mm Schott GG 13 + 0.7mm Schott BG 12 + 5mm of 40% saturated sol. at 0°C of Cu $SO_4 \cdot 5 H_2O$ in a liquid cell* with two quartz windows.
V	2.2mm Schott GG 11 + 1.6mm Schott BG 18.
r	2.0mm Schott RG 1.

*For details of cell construction see Lasker (1966).

The effective wavelengths and relative responses of the V and r filters, which were used for the galaxy observations, have been calculated for two cases. In the first case, a flat spectrum (constant flux per unit wavelength interval)

was assumed, and in the second case, the spectrum of an elliptical galaxy (Oke and Sandage, 1968) was used. For both cases, and for each filter, the transmission of the atmosphere (Allen, 1963a) and two aluminum reflections (Allen, 1963b) were included along with the manufacturer's spectral response function of a typical ITT fw-130 photomultiplier and the filter transmissions which were measured in the Mt. Wilson laboratory. The relative response as a function of wavelength is shown in Figures 1 and 2 for both the V and r filters. In the figures, the integrated responses of the V filters have been normalized so that they are equal. The r filters are on the same relative response scale as their corresponding V filters. The effective wave lengths of the V and r filters are given in Table 3.

TABLE 3

Vr EFFECTIVE WAVELENGTHS

Filter	Galaxy		Flat Spectrum	
	λ	$(1/\lambda)^{-1}$	λ	$(1/\lambda)^{-1}$
V	5407	5425	5383	5400
r	6728	6760	6730	6762

The photoelectric observations were made at the Newtonian foci of the 60" and 100" Mt. Wilson reflectors with a magnetically shielded ITT fw-130 photomultiplier (S-20 surface) which was enclosed in a vacuum insulated "cold-box" and

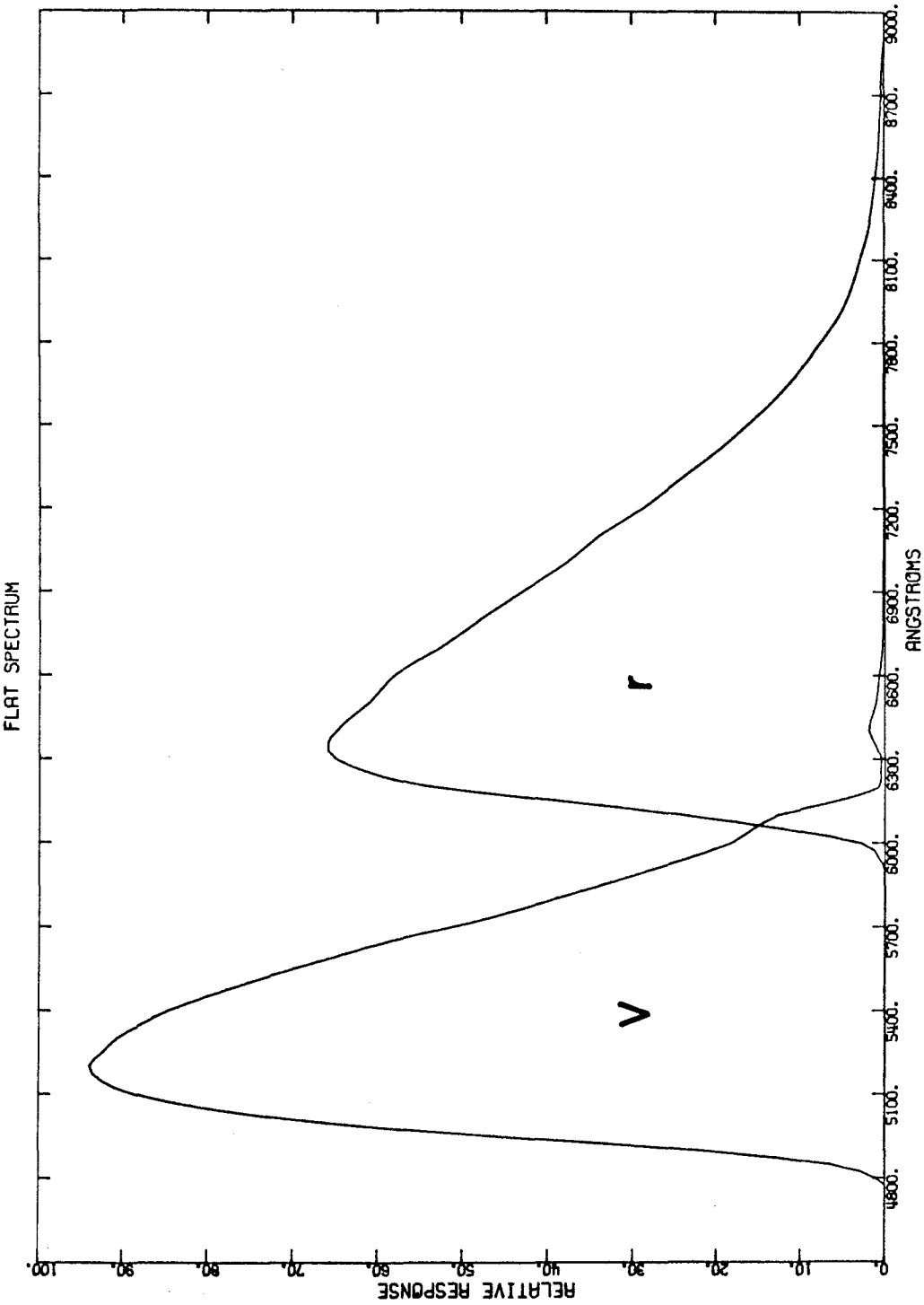

Figure 1 Response of the photometric system to a flat spectrum

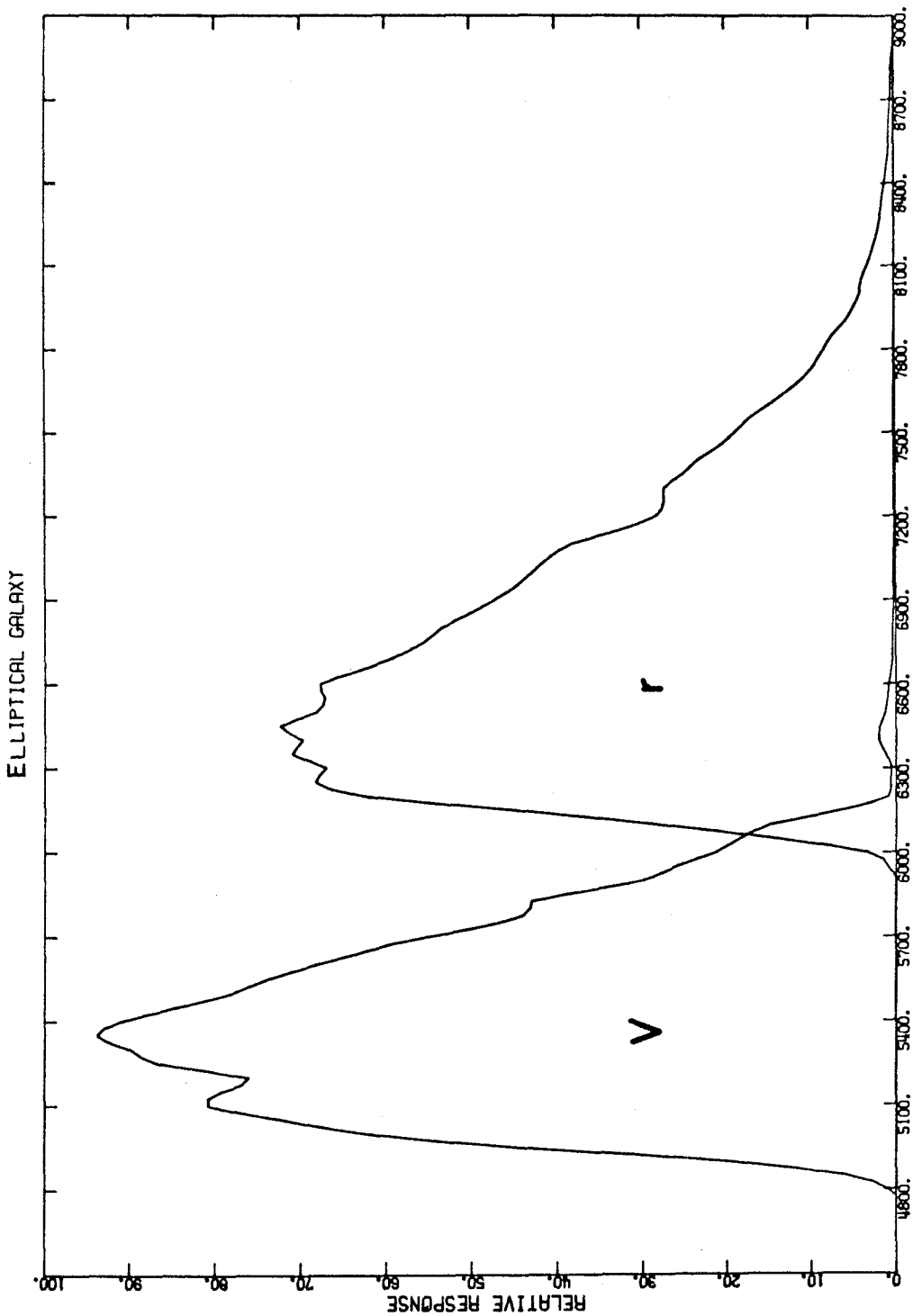

Figure 2 Response of the photometric system to the spectrum of an elliptical galaxy

cooled with dry ice. The pulses from the tube were amplified by a pre-amplifier attached to the cold-box, and then sent to an amplifier and discriminator mounted on the telescopes or on the Newtonian platform. Four different types of readouts were used to monitor and record the observations. First, a frequency meter displayed the instantaneous counting rate and also generated an audio signal of a pitch proportional to the instantaneous counting rate. This allowed the immediate detection of irregularities. Second, a pulse counter was used which displayed the total accumulated counts as the counting proceeded. Third, the total counts for each measurement were printed on a paper tape, and at the 100" they were also recorded on punched cards. Fourth, the total counts of the previously completed measurement were converted to an analogue signal which was used to drive the pen of a strip chart recorder. Thus, the recorder displayed a series of object and sky measurements which could be compared at a glance while the observations were in progress, and it provided an accurate means of determining the sidereal time of each observation, as well as a handy place for writing notations. This data system was designed and built by Dr. E. Dennison and his staff, in the Mt. Wilson and Palomar Observatory's Astro Electronics Laboratory.

The observations of the galaxies were made with the V and r filters. In these pass bands, the flux emitted by a

galaxy is a slowly varying function of wavelength, while in the U and B pass bands, the emitted flux is rapidly declining at shorter wavelengths, and the large H and K absorption lines of Ca II affect the flux in both the U and B bands. For galaxies with increasing redshifts, the H and K lines are shifted further into the B pass band. This causes the total flux received in the B pass band to drop rapidly and makes the B-V and U-B colors a strong function of the redshift.

To minimize the uncertainties involved in correcting for the effects of different redshifts, the V-r colors were used, since the necessary corrections are much smaller than those which would have been required if B-V or U-B colors had been used. The V and r band passes have the additional advantage that the emitted fluxes are higher and the sky backgrounds are lower than in the U and B bands.

In order to determine the atmospheric extinction, four-color observations, UBV and r, were made on a set of standard stars throughout the night. All the objects were visually centered in a diaphragm at the focus of the telescope, and a series of measurements were made, first on the object, and then on an adjacent region of sky. In most cases the time elapsed between the object and the sky measurements was less than 60 seconds. This procedure was repeated until enough counts had been obtained to reduce the statistical error in the observation to less than two per cent. Because long integration times were required for the observations made

with the large diaphragms, only the V filter was used for these in an effort to minimize the telescope time required. Thus, the V-r colors are not available as far from the center of the galaxies as are the V magnitudes.

In order to relate the photometric observations of the brightest galaxy in each cluster to intrinsic properties of the galaxies, magnitudes in Table 4 are the integrated magnitudes of an area of angular diameter θ, which is the angular diameter of an object with a linear diameter of twenty kiloparsecs at the distance where the cosmological redshift is equal to the redshift observed for the galaxy in question. (See Appendix 2 for the formulae used to compute θ). Thus, with the assumption that the distance of the observed galaxy is indicated by its redshift, z, we may interpret the magnitudes in Table 4 as the apparent magnitude of the central 10 kiloparsecs of the galaxy. No attempt has been made to correct for the effects of different ellipticities. The colors in Table 4 are those at $1/2\,\theta$ since the colors were not measured for all the galaxies out to an angular diameter of θ. The observations for NGC 383 are plotted in Figure 3 as a function of diaphragm diameter in seconds of arc. The angular diameters θ and $1/2\ \theta$ are indicated for the V magnitude and the V-r color, respectively.

Table 4

Integrated Colors and Magnitudes

Cluster	V	V-r	θ	Description
76	13.83	0.86	38.9	prominent elliptical
119	14.28	0.84	33.4	prominent elliptical with satellites
147	14.74	0.85	33.6	elliptical with close companion
151	14.29	0.84	28.6	double galaxy
194	12.34	0.79	79.7	double galaxy
262	12.54	0.82	84.3	spiral? (corrected for superimposed star)
278	15.95	0.91	17.7	elliptical with close satellites
347	12.61	0.83	80.1	prominent elliptical (corrected for superimposed star)
376	14.72	0.88	30.7	prominent elliptical
400	13.21	0.94	64.6	double galaxy
407	14.70	0.91	31.5	composite galaxy
426	12.13	0.81	78.0	Seyfert galaxy, superimposed star
505	14.43	0.90	27.8	prominent elliptical
539	13.74	0.87	53.9	S most in chain of three ellipticals
548	14.13	0.86	37.6	W most elliptical in central pair
553	15.44	0.93	23.0	prominent elliptical
568	15.50	0.87	20.1	elliptical with close companions
569	12.71	0.85	73.7	prominent elliptical
576	14.37	0.86	36.5	SE most elliptical in central pair
592	15.20	0.80	24.6	SE most elliptical in central pair
634	13.61	0.85	54.1	prominent elliptical (non central)
671	14.23	0.86	30.1	prominent elliptical with satelites
754	14.34	0.86	28.1	elliptical with close companion
779	13.22	0.78	70.8	double galaxy
993	14.48	0.85	28.4	prominent elliptical
1060	11.60	0.82	122.0	NW most elliptical in central pair
1139	14.20	0.81	39.0	elliptical with close companion
1185	13.58	0.81	41.8	double galaxy
1213	14.24	0.79	50.3	elliptical (non central)
1228	14.10	0.78	42.4	E most elliptical in central pair
1257	14.52	0.83	43.0	elliptical with close companion
1314	13.65	0.81	43.5	spiral?
1318	12.75	0.74	75.2	S0 or spiral edge on
1367	12.56	0.76	69.8	prominent elliptical with satellites
1377	14.73	0.80	29.3	elliptical with close companion
1656	12.69	0.77	63.0	E most elliptical in central pair, with satellites
1736	14.33	0.89	34.4	prominent elliptical
2052	13.83	0.86	41.6	elliptical with close companion
2147	13.86	0.81	41.6	prominent elliptical
2151	14.04	0.77	42.1	prominent elliptical
2152	14.40	0.81	33.7	elliptical with close companion
2162	13.48	0.80	45.7	prominent elliptical
2197	13.20	0.82	45.1	prominent elliptical
2199	13.02	0.77	45.0	composite galaxy
2319	14.78	0.89	27.5	prominent elliptical
2634	13.22	0.85	46.4	double galaxy
2657	14.77	0.88	35.3	elliptical
2666	12.95	0.78	52.8	prominent elliptical
03+3909	13.16	0.89	83.8	prominent elliptical
22+3552	13.05	0.82	69.8	prominent elliptical
01+3300	11.96	0.81	90.6	elliptical with close companion
01+3209	12.17	0.86	80.6	elliptical with close companion
01+0523	12.14	0.82	75.6	elliptical with close companion
04-0511	11.64	0.80	87.8	elliptical with satellites
22+3505	13.28	0.81	50.9	prominent elliptical

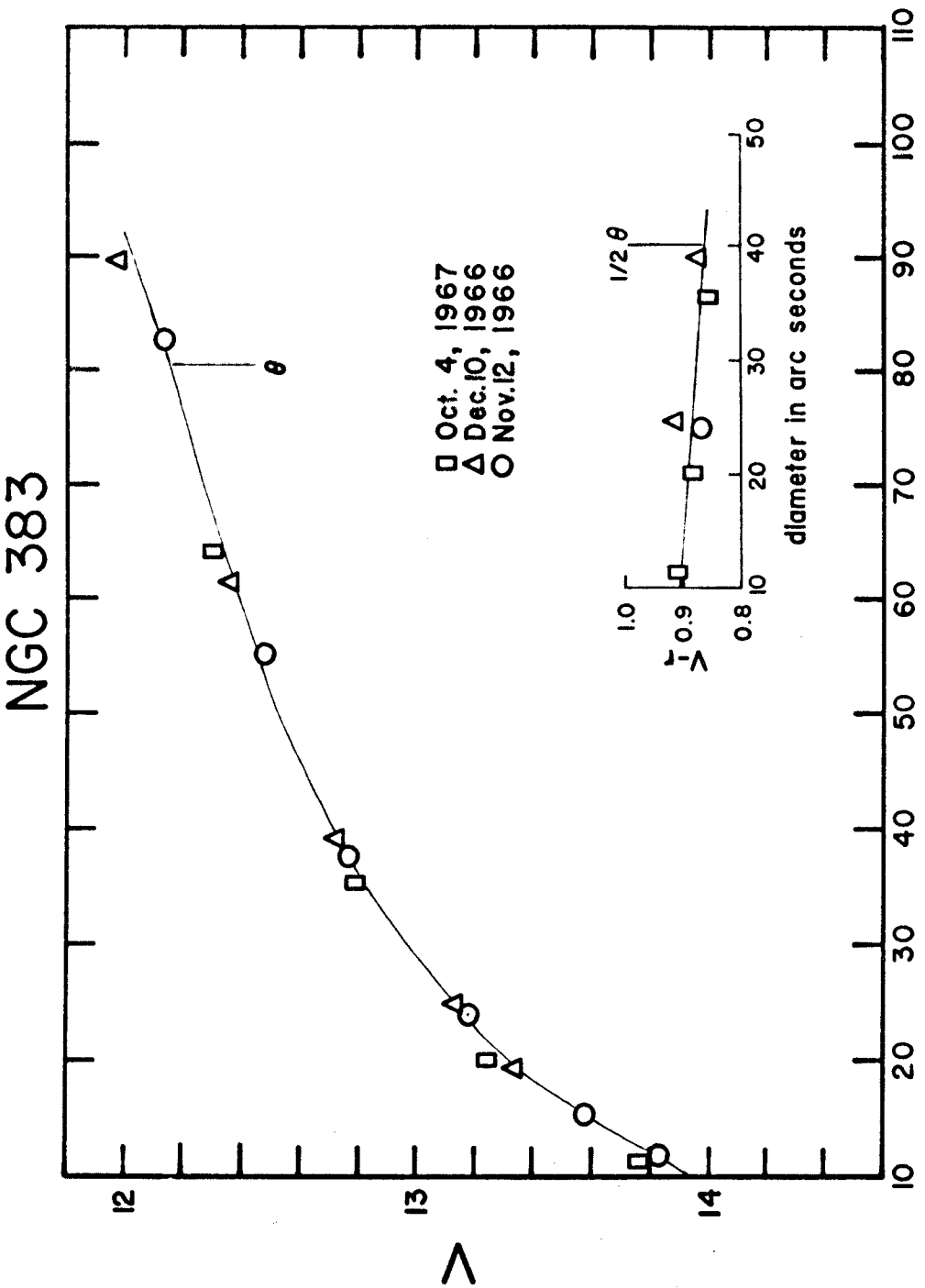

Figure 3 Integrated magnitudes and colors vs. diaphragm diameter in seconds of arc

Redshift Measurements

The redshifts for the majority of the program clusters were measured from 190A/mm plates that were taken by Professor M. Schmidt with the Cassegrain image-tube spectrograph on the 200" Hale telescope. Although the dispersion of the image-tube plates is non-linear, it is a smoothly varying function of wavelength, and can be accurately determined from the measurements of the comparison lines on the plate. Figure 4 illustrates the cubic term in the variation of the dispersion with wavelength.

The measurements of all of the plates were made with the Grant photoelectric spectrum comparator at the California Institute of Technology, which records each measurement, along with an estimate of the type and strength of the line measured, on punched cards. These cards were used by an IBM 7090/94 as input data for computing the wavelength calibration curve, and for converting the measurements of the screw positions to wavelengths. The calibration curve was obtained from a least-square fit of a third order polynomial to the measurements of the comparison lines. For a typical plate the standard deviation of the wavelength of a line is 0.5A.

The systematic velocity error introduced by the curvature of the spectral lines was determined from measurements of a specially prepared plate which had the Helium

and Argon comparison spectra in the area where the galaxy spectrum normally was, as well as in the area normally used for the comparison spectra. An average systematic correction of -25 km/sec was adopted.

The measured redshift, z, of the brightest galaxy in each cluster is given in Table 5 unless noted otherwise. Here, 1 + z is defined as the ratio of the observed to the emitted wavelength. All the redshifts in the first column have been reduced to the sun. In the second column the redshifts have been reduced to the local group using a solar motion of 300 km/sec in the direction of the point at new galactic coordinates b = 0°, l = 90°.

As can be seen from the list of identified features in column 4 of Table 5, 9 out of 55, or 16% of the objects have emission lines in their spectra.

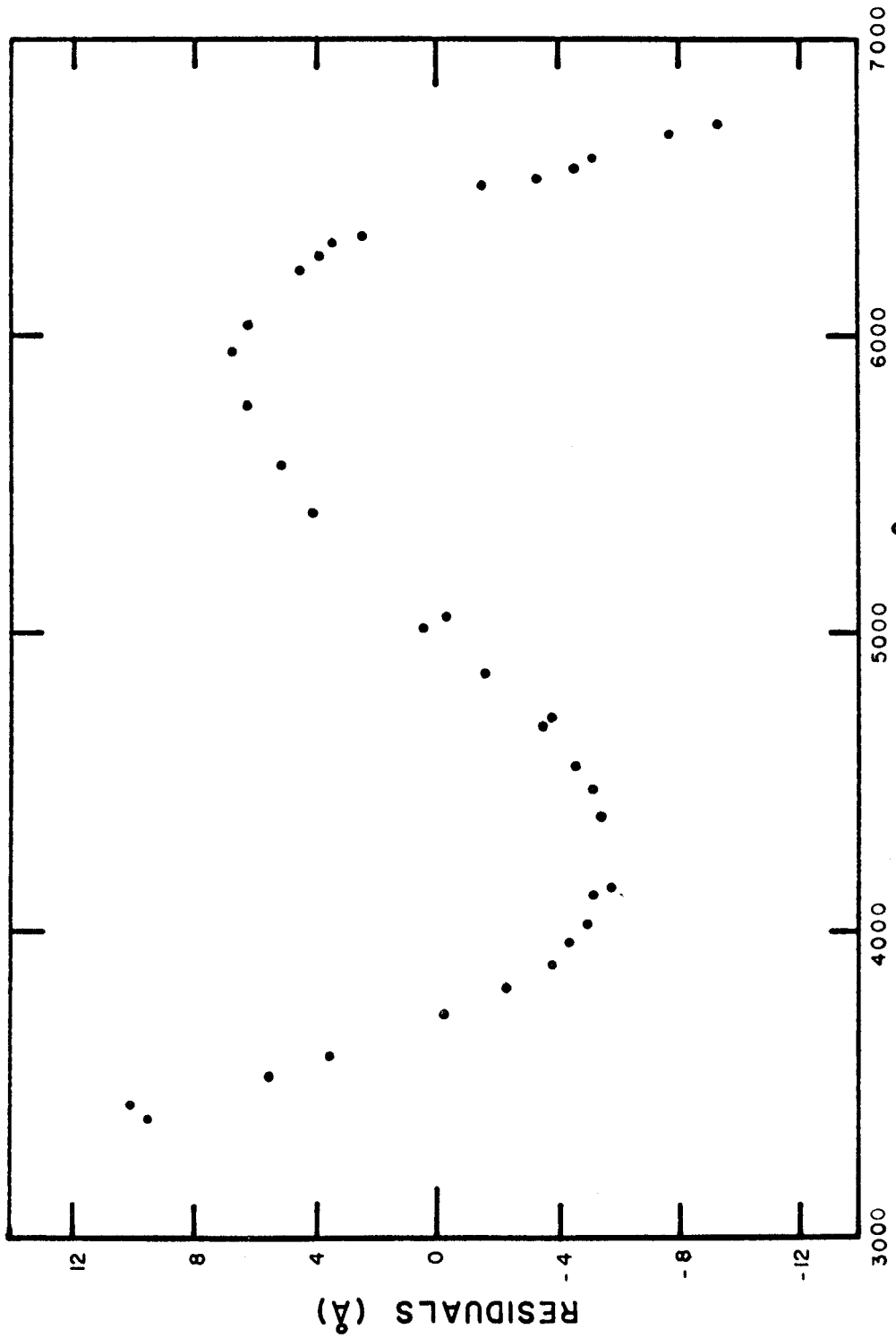

Figure 4 Residuals to a second-order wavelength calibration curve for Palomar image-tube plate Q19

Table 5

Redshifts

Cluster	Z_{sun}	Z	Identified Lines	
76	.0372	.0377	abs.H,K,G,MgH	
119	.0440	.0444	abs.H,K,G,MgH,FeI	*
147	.0437	.0441	abs.H,K,G,MgH	
151	.0525	.0526	abs.	*
194	.0175	.0178	abs.	*
262	.0161	.0168	em.3727 abs.H,K,G,FeI,MgI,MgH,NaI	
278	.0897	.0904	abs.H,K,G	
347	.0171	.0177	abs.H,K,G,FeI,MgI,NaI	*
376	.0482	.0487	abs.H,K,G,MgH	
400	.0230	.0231	abs.H,K,G,MgI,FeI	*
407	.0469	.0473	abs.H,K,G,MgI	*
426	.0177	.0182	em.	*
505	.0535	.0543	abs.H,K,G	*
539	.0270	.0267	abs.H,K,G,FeI	
548	.0399	.0391	abs.H,K,G,FeI,MgH	
553	.0667	.0670	abs.H,K,G,MgI	
568	.0780	.0780	abs.	*
569	.0192	.0193	abs.H,K,G,FeI,MgI,NaI	
576	.0401	.0404	abs.H,K,G,MgI,MgH	*
592	.0626	.0621	abs.H,K,G,FeI,H	*
634	.0263	.0266	abs.H,K,G	
671	.0499	.0497	abs.H,K,G,MgI	
754	.0545	.0537	abs.H,K,H	*
779	.0202	.0201	abs.	*
993	.0538	.0530	abs.H,K,G	
1060	.0124	.0115	abs.H,K,G,MgI	*
1139	.0382	.0376	abs.H,K,G,MgI	
1185	.0351	.0349	abs.H,K,G,MgI,FeI	*
1213	.0289	.0287	em.3727, [OIII] abs.H,K,G,MgI,FeI	
1228	.0345	.0344	abs.H,K,G,MgH,NaI,Hδ,Hγ	

* see notes to table

Table 5 (contd.)

Cluster	Z_{sun}	Z	Identified Lines	
1257	.0340	.0339	em.3727 abs.H,K,G,MgI,MgH,NaI	
1314	.0333	.0335	abs.H,K,G,MgI,NaI	
1318	.0186	.0189	abs.H,K,G,MgI,MgH,NaI	
1367	.0206	.0204	abs.K	*
1377	.0509	.0512	abs.H,K,G,MgI	*
1656	.0227	.0227	abs.	*
1736	.0438	.0431	abs.H,K,MgH,FeI	
2052	.0350	.0351	em.	*
2147	.0348	.0351	abs.G,MgI	*
2151	.0343	.0347	abs.	*
2152	.0436	.0440	abs.H,K,G	
2162	.0313	.0318	abs.H,K,G,FeI,MgH	*
2197	.0315	.0322	abs.H,K,G,FeI,MgI,MgH	*
2199	--	.0316	em.	*
2319	.0539	.0549	em.3727, [OIII] abs.H,K,G,FeI,Hδ,Hγ	
2634	.0305	.0313	em.3727 abs.H,K,G,MgI,MgH	*
2657	.0408	.0414	abs.H,K,G,FeI,MgH,MgI	*
2666	.0265	.0273	abs.H,K,G,MgI,MgH,FeI	
03+3909	.0165	.0169	em.3727,Hβ abs.H,K,G,MgI,NaI,MgH	
22+3552	.0194	.0204	abs.H,K,G,MgI,MgH	
01+3300	.0149	.0156	abs.	*
01+3209	.0169	.0176	abs.	*
01+0523	.0185	.0188	abs.	*
04-0511	.0164	.0161	abs.	*
22+3505	.0275	.0284	abs.H,K,G,MgI,FeI,MgH	

* see notes to table

Notes to Table 5

119 3C29 Z_{sun}=.0447 Sandage, A.R. Ap.J.,150,L145

151 HMS cluster 0106+1536; average of 2 brightest

194 3C40 Zwicky et. al., Catalogue of Clusters of Galaxies, Vol.5, cluster 0123-0138, average of 4

347 3C66 may be outlying member: Z=.0215 Mathews, Morgan, and Schmidt Ap.J.,137,153

400 3C75; double galaxy, redshift is average of two measured on the same plate.

407 4C35.6; multiple nuclei in one halo, or compact cloud of galaxies. Redshift is average of two NW most condensations measured on the same plate.

426 Perseus Cluster; 3C84=NCG 1275 is brightest member and shows emission. Redshift is average of 5 from HMS

505 90 A/mm plate

568 HMS cluster 0705+3506; average of 2 brightest

576 redshift for 2nd brightest at 7 18 01 +55 58.2 1950

592 90 A/mm plate

754 90 A/mm plate

779 HMS group 2832; average of 2

1060 redshift for 2nd brightest at 10 34 19 -27 15.1 1950 coordinates

1185 redshift is that of strong NE stellar component

1367 400 A/mm 100" plate, average of brightest galaxy and near companion on same plate. 3C264=NGC 3862 may be an outlying member: Z=.0206 Schmidt, M., Ap. J.,141,1

1377 redshift for 2nd brightest at 11 45 18 +56 02.0 1950 coordinates

1656 Coma Cluster; average of NGC 4889 and NGC 4874 from HMS

Notes to Table 5 (contd.)

2052 3C317; Z=.0350 Schmidt,M., Ap.J.,141,1 three condensations in single envelope

2147 redshift is average of two plates. The galaxy is underexposed and the night sky is strong on both plates.

2151 Hercules Cluster; redshift is average of 3 brightest from HMS

2152 no comparison lines on plate. wavelength scale of previous plate used with night sky emission lines as a check

2197 redshift of 2nd brightest at 16 25 55 +41 01.7 1950 coordinates

2199 3C338; Z=.0316 Minkowski,R., A.J.66,558

2634 3C465; Z=.0293 Schmidt,M., Ap.J.141,1

2657 average of 2 brightest:1st Z=.0413 abs. K,G,MgI 2nd Z=.0405 abs.H,K,G,FeI,MgH 23 42 21 +08 54.7 1950 coordinates

01+3300 HMS group 507; average of 3

01+3209 HMS group 383; average of 3

01+0523 HMS group 741; redshift of NGC 741

04-0511 HMS group 1600; average of 2

HMS - Humason,M.L.,Mayall,N.U.,and Sandage,A.R.,A.J.,61,97

III. DISCUSSION

Introduction

The absolute magnitudes and colors, which were computed from the redshift and the apparent magnitudes and colors, have been used to derive the absorption and color-excess produced by the material in the galactic plane. It was assumed that, on the large, the absorbing material is distributed in plane parallel layers. The absorption in magnitudes is then a linear function of cscb.

However, the values found for the absorption and color-excess are lower limits because only the brightest clusters have been selected for study. Consider, for example, two equal areas of sky, the first being unobscured, and the second being obscured by one magnitude. The average obscuration of the two areas together is 0.5 magnitude. However, since the number of visible objects down to some limiting magnitude is proportional to $10^{0.6m}$ (if the objects are uniformly distributed in space) there will be $10^{0.6m}/10^{0.6(m-a)} = 10^{0.6a}$ or approximately four times as many objects visible in the unobscured area as in the obscured area. As a result, the absorption calculated by giving equal weights to each object would be 0.2 instead of 0.5. The correct result obtains when each object is given a weight which is proportional to the reduction in number caused by the presence of the absorbing material, namely $10^{0.6a}$, where a is the amount of absorption,

in magnitudes, which occurs.

It is interesting to note that if the sample is incomplete, the result will not be affected as long as the incompleteness occurs because some of the objects were missed at random. This is because the ratio of the number of objects in the absorbed area to the number of those in the unabsorbed area is maintained.

Two cases for the distribution of the absorbing material have been considered. For Case I, the absorbing material was taken to be distributed smoothly in plane parallel layers. For Case II, the absorbing material was taken to be distributed in patches which, on the large, had a plane parallel distribution. In each case the objects were given a weight equal to $10^{0.6a}$, where a was the absorption appropriate to the object, and a solution was made for the linear regression curve by the method of least squares. The ratio of the absorption found using equal weights to the absorption found using a weight of $10^{0.6a}$ may be considered as the fraction of the true absorption which is found by simply taking equal weights. The two cases considered give two estimates of this fraction.

The galaxy counts of Shane and Wirtanen (1967) have been used to determine how representative the areas around the clusters are of the entire sky. As expected from the sample above, the areas around each cluster show less absorption than the sky as a whole.

A cloud model for the absorbing material (see Appendix 3) has also been used to calculate the amount by which the absorption is underestimated.

Absolute Magnitudes and Colors

The apparent magnitudes and colors in Table 4 have been transformed into absolute magnitudes and colors with the following equations:

$$M_V = m_V - 5 \log p + 5 - K_V \qquad (1)$$

$$C_{V-r} = c_{V-r} - K_{V-r} \qquad (2)$$

M and C are the absolute magnitude and color. m and c are the apparent magnitude and color. K is the "K-correction" which corrects for the effects of the relative velocities of the observer and the source. p is the "distance" in parsecs between the observer and the source and depends upon the cosmological model as well as upon the redshift. The equations used for computing K (z) and p (z) are discussed in Appendix 2.

In Table 6, the values of p, K, and θ are given for various values of z. These are based upon the K- corrections of Oke and Sandage (1968) and upon the zero pressure, zero cosmological constant solution of the Einstein equations (assuming spacial isotropy) with $c/H_o = 3 \times 10^9$ parsecs and $q_o = 1/2$.

TABLE 6

z	p	K_V	K_{V-r}	θ
.01	30	0.040	0.009	139.9
.02	59	0.083	0.020	71.2
.03	88	0.129	0.034	48.3
.04	117	0.175	0.050	36.8
.05	145	0.222	0.066	30.0
.06	172	0.267	0.080	25.4
.07	200	0.308	0.091	22.1
.08	226	0.347	0.100	19.7
.09	253	0.387	0.110	17.8
.10	279	0.427	0.120	16.3

p is in megaparsecs

θ is in seconds of arc

The Cscb Dependence of the Absolute Magnitudes and Colors

The absolute magnitudes and colors are given in Table 7 along with the value of cscb for each galaxy. In Figure 5 and Figure 6, the absolute magnitudes and colors have been plotted vs. cscb. Also shown in the figures are the linear regression curves estimated by the method of least squares with each point having equal weight. The equations for the regression lines are:

$$M_V = M_V^o + A\text{cscb} \tag{3}$$

$$C_{V-r} = C_{V-r}^o + E\text{cscb} \quad . \tag{4}$$

Here, A is the absorption suffered by an object at the galactic pole and M_V^o is the average absolute magnitude of the brightest cluster galaxy. Similarly, E is the color-excess of an object at the galactic pole and C_{V-r}^o is the average color of the brightest cluster galaxy. The values of the coefficients and their errors are given in the first line in Table 8.

The ratio of total to selective absorption, R, is given by:

$$R = A/E \tag{5}$$

Combining equations (3) and (4) we obtain:

$$M_V = M_V^o - R\, C_{V-r}^o + R\, C_{V-r} \tag{6}$$

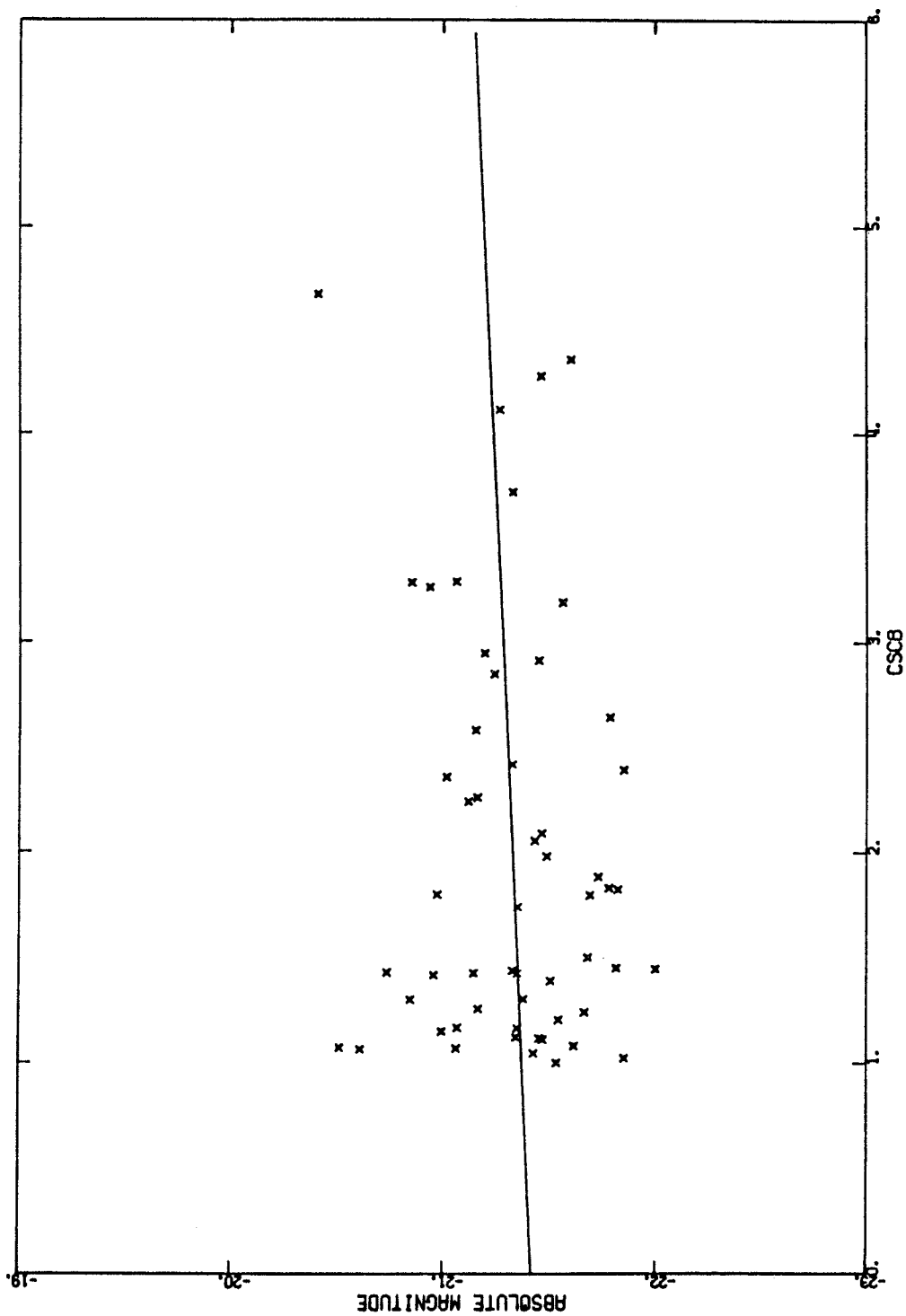

Figure 5 M_V vs. cscb

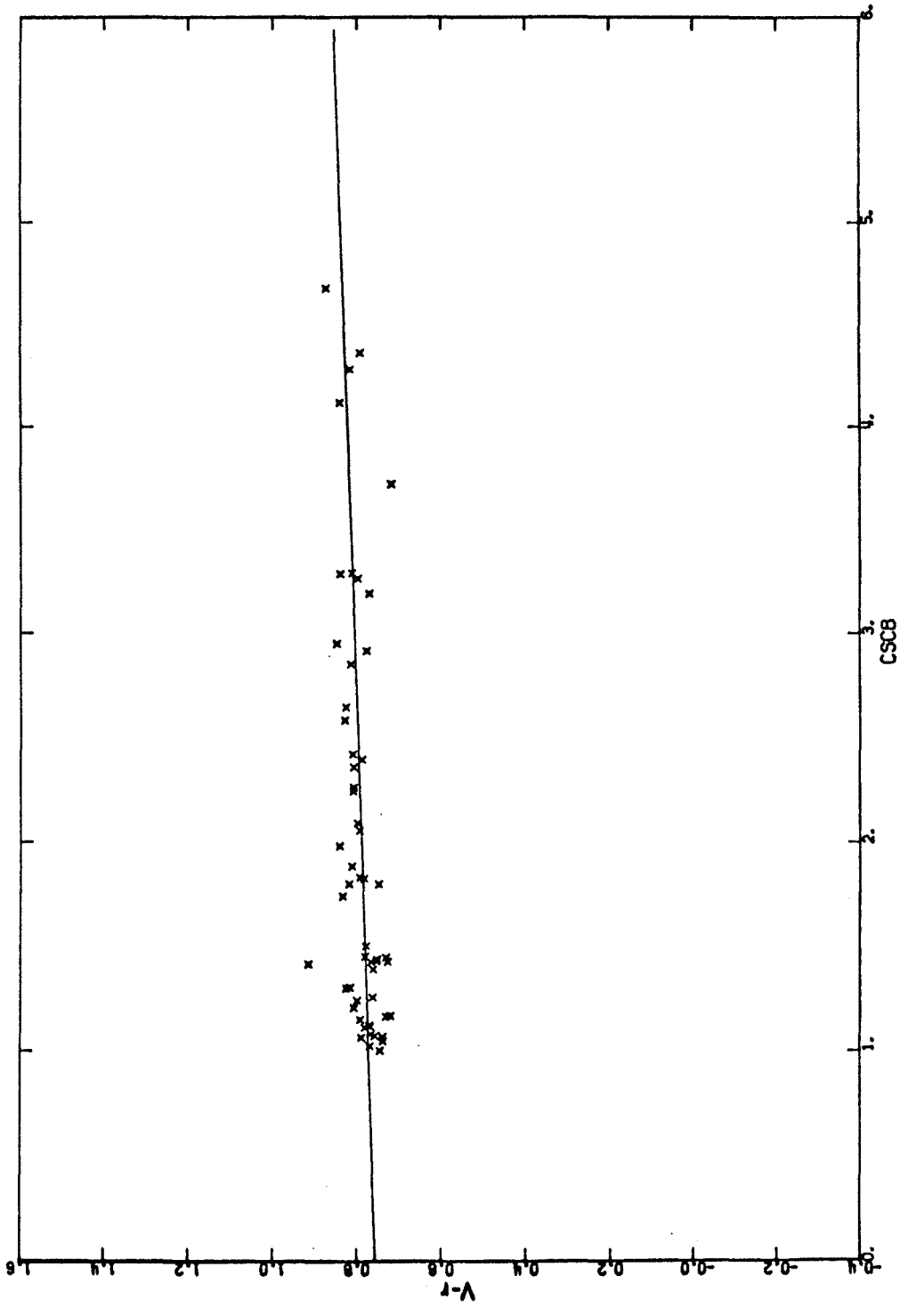

Figure 6 C_{V-r} vs. cscb

Table 7

Absolute Magnitudes and Colors

Cluster	cscb	V	V-r
76	1.206	-21.54	0.81
119	1.112	-21.47	0.78
147	1.150	-20.99	0.79
151	1.024	-21.85	0.77
194	1.123	-21.34	0.77
262	2.358	-21.01	0.81
278	2.090	-21.46	0.80
347	3.289	-21.06	0.81
376	2.850	-21.24	0.82
400	1.416	-20.95	0.92
407	2.934	-21.19	0.85
426	4.360	-21.60	0.79
505	2.643	-21.78	0.83
539	3.285	-20.85	0.84
548	2.418	-21.33	0.81
553	4.117	-21.27	0.84
568	3.190	-21.56	0.77
569	2.581	-21.15	0.83
576	2.260	-21.16	0.81
592	3.720	-21.33	0.72
634	1.798	-20.97	0.82
671	1.830	-21.78	0.80
754	2.393	-21.85	0.79
779	1.429	-20.73	0.76
993	1.052	-21.68	0.78
1060	2.242	-21.12	0.81
1139	1.256	-21.16	0.76
1185	1.081	-21.62	0.77
1213	1.072	-20.51	0.76
1228	1.068	-21.06	0.74

Table 7 (contd.)

Cluster	cscb	V	V-r
1257	1.064	-20.61	0.79
1314	1.117	-21.45	0.77
1318	1.167	-21.07	0.72
1367	1.046	-21.43	0.74
1377	1.165	-21.35	0.73
1656	1.001	-21.53	0.75
1736	1.740	-21.35	0.84
2052	1.303	-21.38	0.82
2147	1.426	-21.35	0.77
2151	1.426	-21.14	0.73
2152	1.439	-21.33	0.75
2162	1.390	-21.50	0.76
2197	1.452	-21.81	0.78
2199	1.447	-22.00	0.73
2319	4.279	-21.46	0.82
2634	1.833	-21.73	0.81
2657	1.303	-20.84	0.83
2666	1.797	-21.69	0.75
03+3909	4.675	-20.41	0.87
22+3552	3.262	-20.94	0.80
01+3300	2.054	-21.43	0.80
01+3209	1.980	-21.49	0.84
01+0523	1.241	-21.66	0.80
04-0511	1.824	-21.82	0.77
22+3505	2.914	-21.45	0.78

Equation (6) shows that R could be obtained directly from the regression of M_V on C_{V-r} if C_{V-r} were error-free. Since neither M_V nor C_{V-r} may be considered error-free, the true value of R will be bounded by the values determined from the regression of M_V on C_{V-r} and from the regression of C_{V-r} on M_V (which yields a value for 1/R). We see from Table 8 that the errors in M_V are ten times those in C_{V-r}. Thus, the true value of R will most likely be closest to that obtained from the regression of M_V on C_{V-r}. The results are shown in the first line of Table 9.

Case I - Smooth Layers

Let us assume that the absorbing material is smoothly distributed in plane parallel layers. The absorption, a, at each point would then be a=Acscb where A is the amount of absorption at the galactic pole. The value of A was found by choosing a trial value, computing the weights, $10^{0.6Acscb}$, and then comparing the trial value with the coefficient of the regression curve of M_V on cscb. The same weights were used in estimating the regression curve of C_{V-r} on cscb in order to determine the color-excess, and in estimating the regression curves of M_V on C_{V-r} and C_{V-r} on M_V in order to determine bounds on the ratio of total to selective absorption. Results are given on the second line in Tables 8 and 9.

Taking the absorption found by using the weights

Table 8

REGRESSION COEFFICIENTS

	M_V on cscb					C_{V-r} on cscb				
ERMS	M_V^o	e	A	e	ERMS	C_{V-r}^o	e	E	e	Case
0.35	-21.41	0.11	0.045	0.049	0.036	0.76	0.01	0.017	0.005	equal weights
0.35	-21.43	0.11	0.054	0.046	0.037	0.76	0.01	0.016	0.005	smooth layers
0.36	-21.44	0.11	0.068	0.048	0.039	0.77	0.01	0.016	0.005	patchy distribution

ERMS is the root mean-square deviation of a single point
e is the root mean-square error in the coefficient

Table 9

RATIO OF TOTAL TO SELECTIVE ABSORPTION

R from M_V on C_{V-r}	R from A/E	R from C_{V-r} on M_V	Case
2.19	2.72	36.49	equal weights
2.53	3.42	31.66	smooth layer
2.92	4.36	25.36	patchy distribution

$10^{0.6\ Acscb}$, as the best estimate of the true absorption, we find that the solution simply using equal weights gives only 0.66 of the true absorption.

Case II - Patchy Distribution

Let us assume that the absorbing material is distributed in patches which have, in the large, a plane parallel distribution. Thus, the average absorption is given by $\bar{a}$ = Acscb, but at any point the absorption may have any value greater than or equal to zero.

Now, if the brightest cluster galaxy has a unique color or absolute magnitude, and if there were no errors in the colors or absolute magnitudes, then the absorption could be obtained for each point from R times the difference of the "observed" color and the intrinsic color, and from the difference of the "observed" absolute magnitude and the intrinsic absolute magnitude. Using the results obtained with equal weights, we see that the absorption indicated by the dispersion in absolute magnitude is greater by a factor of 2.5 than the absorption indicated by R times the dispersion in color. Since the measuring errors are about the same for the colors and magnitudes, this indicates that the intrinsic dispersion in absolute magnitude is greater than the intrinsic dispersion in color. Therefore, it has been assumed that the brightest cluster galaxy has a unique color, C^{o}_{V-r}, and the

colors, C_{V-r}, have been used to compute the weights, $10^{0.6R[C-C^O]}$.

The value of R was found by choosing a trial value, computing the weights, and then comparing the trial value with the ratio A/E. The same weights were used in estimating the regression curve of C_{V-r} on cscb to determine E, and in estimating the regression curve of M_V on cscb to obtain A. The same weights were also used in estimating the regression curves of M_V on C_{V-r} and C_{V-r} on M_V in order to determine bounds on the ratio of total to selective absorption. The results are given on the third line in Tables 8 and 9.

Taking the absorption found by using the weights $10^{0.6R[C-C^O]}$ as the best estimate of the true absorption, we find that the solution simply using equal weights gives only 0.83 of the true absorption.

Let us examine in more detail the distribution of colors and, thus, the distribution of absorption. In Figure 7 is plotted the weighted number of objects in each interval of color. Here R = 4.0, and only objects with $1.0 \leq cscb \leq 1.6$ have been used. The curve in the figure represents the continuous distribution defined by the points.

It is an unfortunate consequence of the method used here that, even when weights are used to correct for the selection effects, the absorption can still be badly underestimated. This can occur because the sample used is finite, and it is the large absorptions with large weights which have

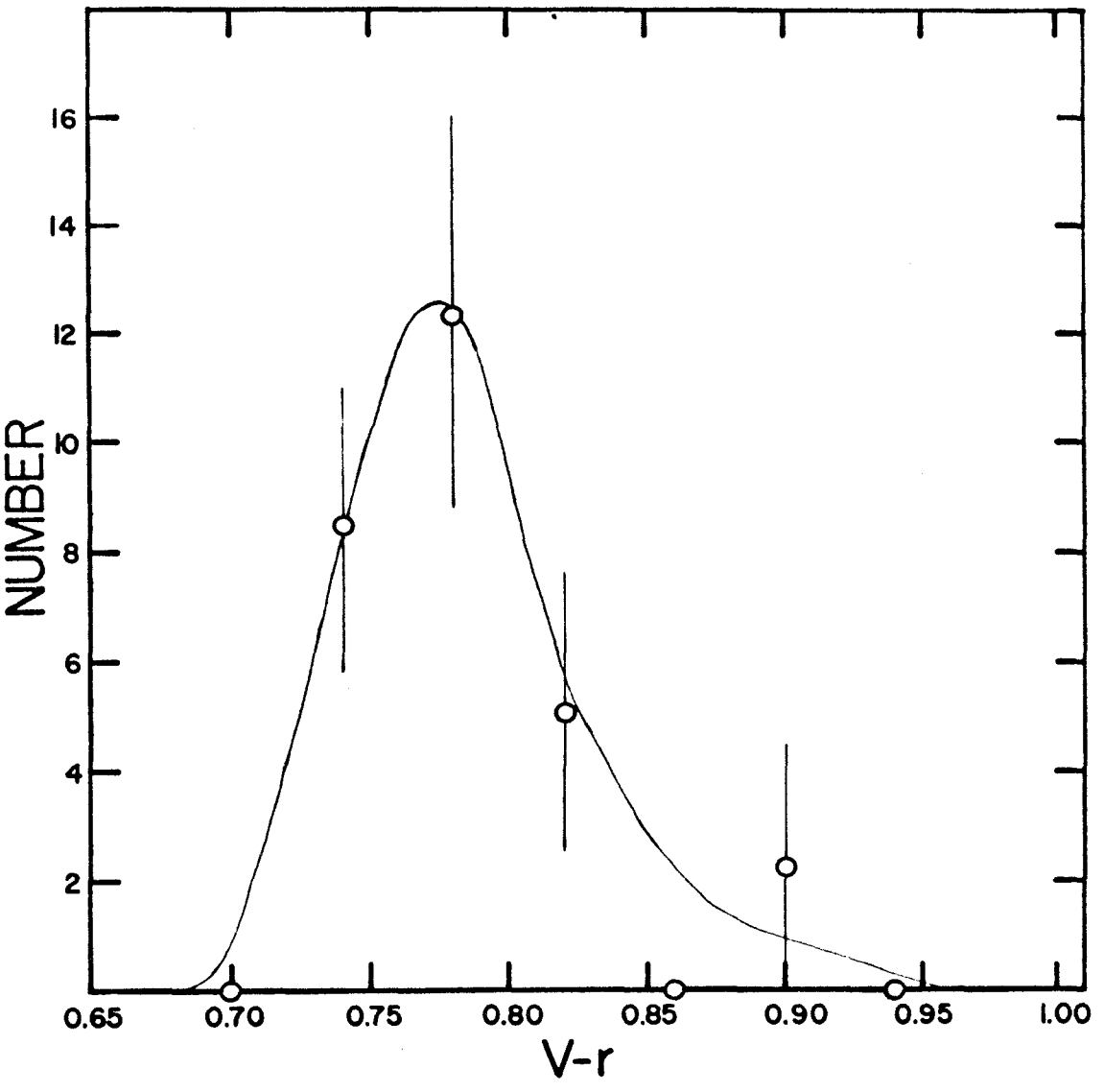

Figure 7 Color distribution

lowest probability of being observed. For example, for most samples of 55 objects, the absorption will be underestimated because a heavily absorbed object is not observed. However, a very few samples of 55 objects will overestimate the absorption by enough to make the average correct (providing, of course, that the heavily absorbed point is not thrown out by the investigator).

This can also be seen from the curve in Figure 7. As drawn in the figure, the color-excess computed from the curve is 0.016 which, as expected for these high latitude objects, is equal to E, the color excess at the galactic pole found from the regression curve. However, if the curve in the figure is extended from its value at a V-r of 0.90 to the abscissa at V-r of 1.10, the color-excess computed from the curve becomes 0.028. In extending the curve, large absorptions having low probability of being observed, have been included. As can be seen from the figure, extending the curve in this manner is quite compatible with the data points. Thus, the finite sample investigated here could underestimate the absorption and color-excess by a factor of two!

Galaxy Counts

The cscb dependence of the galaxy counts of Shane and Wirtanen (1967) in the areas around the clusters has been compared with that for the entire area of sky investigated by

Shane and Wirtanen. They have found that the relation:

$$\log \bar{N} = B - \alpha \text{cscb} \qquad (7)$$

is a good representation of the cscb dependence of the average number of galaxies per square degree, $\bar{N}$.

Using their counts in one-degree squares, and their correction procedures, the average number of counts per square degree for the area of sky in an annulus around each cluster was computed. The angular diameter of the annulus was chosen for each cluster to be the same as the angle subtended by a sphere 8 megaparsecs in diameter at the distance of the cluster. The width of the annulus was one degree. This was done to exclude, as much as possible, the effects of the cluster itself upon the galaxy counts. The results are shown in Figure 8. The line in the figure is the linear regression curve of log $\bar{N}$ on cscb estimated by the method of least squares.

Figure 8 of Shane and Wirtanen (1967) was also used to estimate the average counts per square degree in the region of each cluster. In this case, the average counts per square degree have been smoothed over a much larger area than that enclosed by the annulus in the treatment above. These results are shown in Figure 9. As before, the line in the figure is the regression curve.

Table 10 gives the coefficients, B and α, for the two cases described above, as well as the values found by Shane

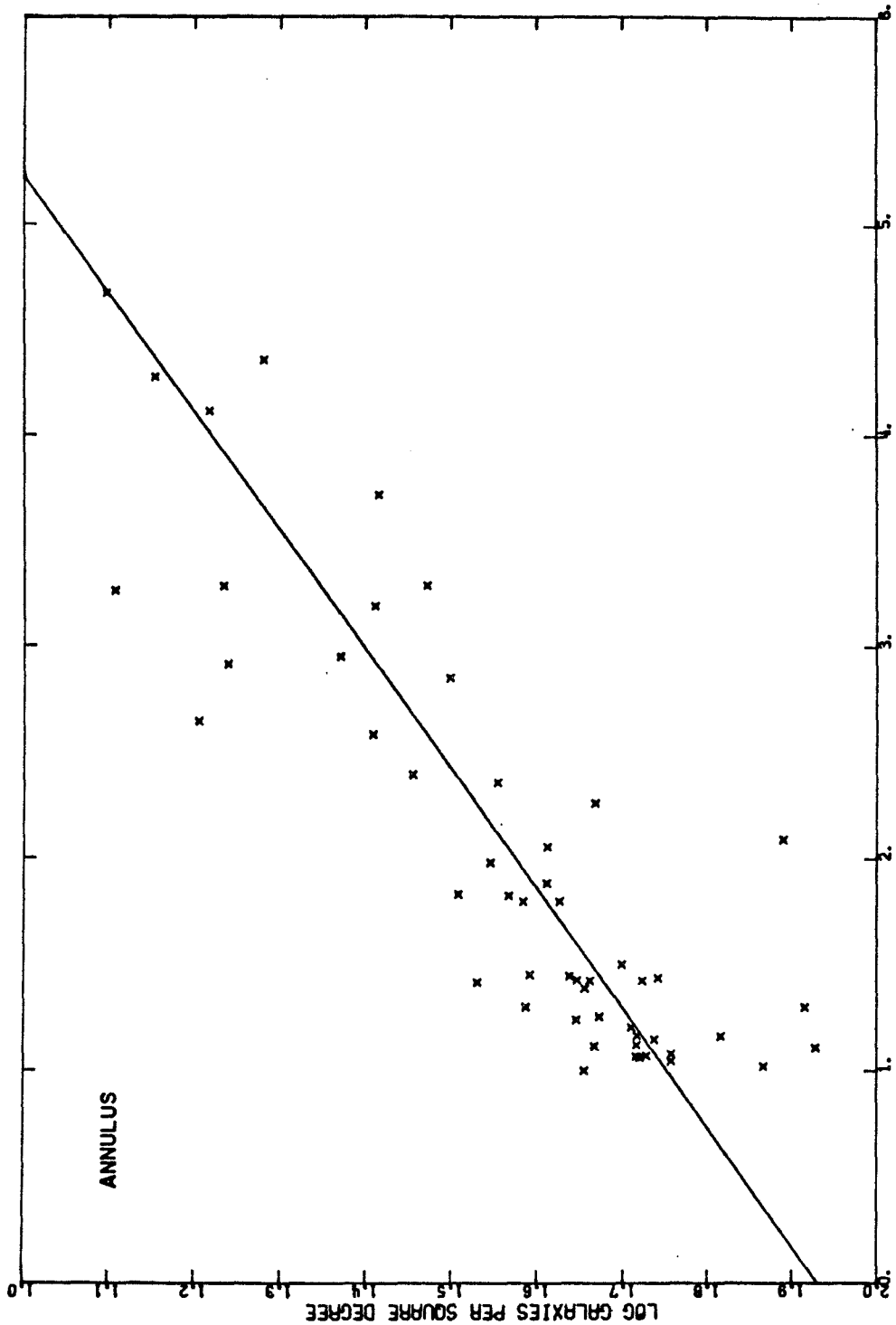

Figure 8 Log of the average number of galaxies per square degree in an annulus vs. cscb

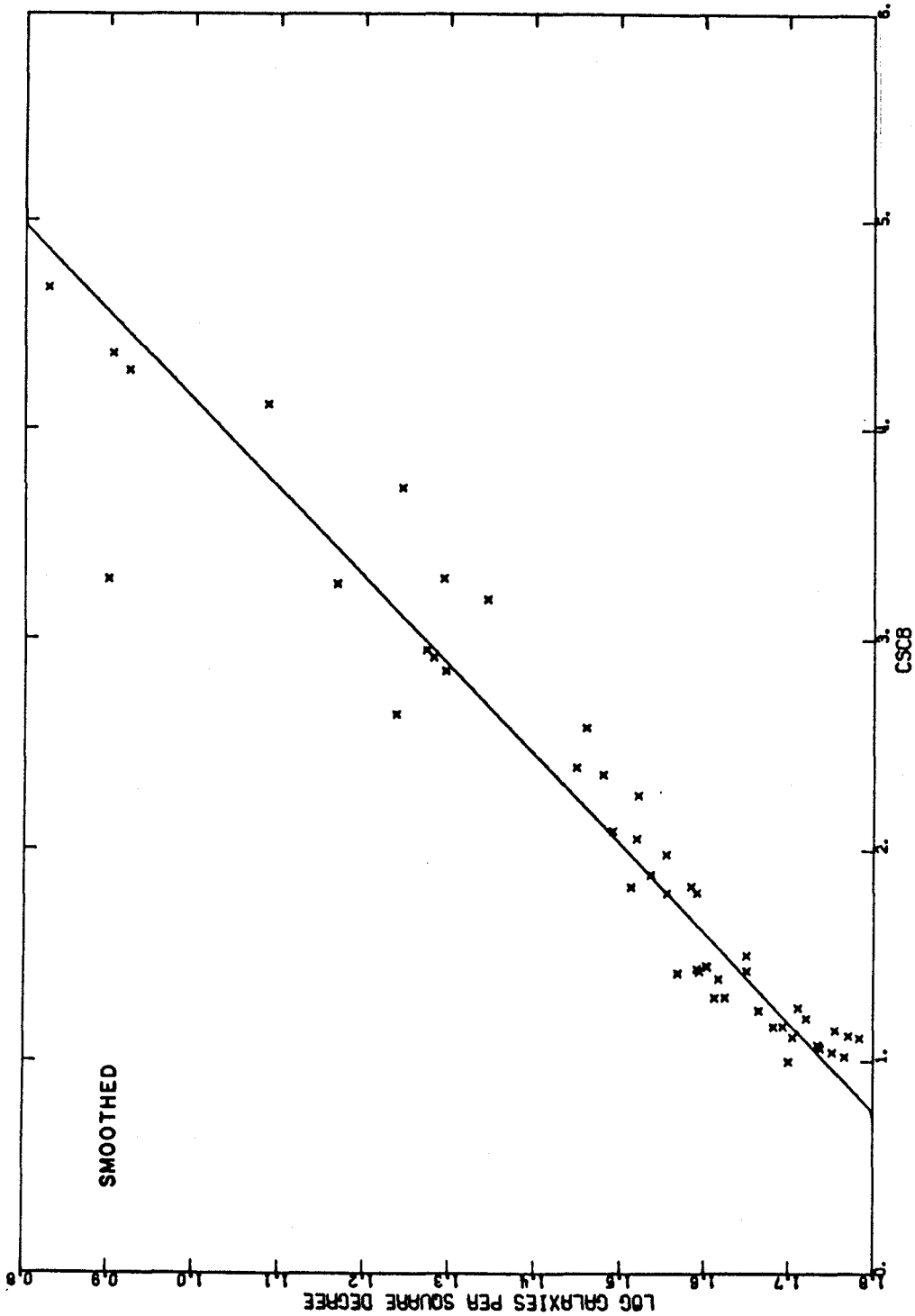

Figure 9 Log of the average number of galaxies per square degree smoothed over a large area vs. cscb

and Wirtanen for the entire sky. The values of α for the smoothed counts and for the entire sky are in good agreement, while the value of α for the counts in the annuluses is less by a factor of 0.75. This indicates that the absorption of a cluster is, on the average, 75% of the average absorption expected at the latitude of the cluster. Taking an average of the fraction of the best estimate of the absorption computed for Case I and Case II we have 0.75, in remarkable agreement with the amount of the underestimate obtained from the galaxy counts.

TABLE 10

GALAXY COUNTS VS. cscb

B	α	Case
1.93	0.178	annulus
1.98	0.237	smoothed
1.95	0.240	entire sky

Cloud Model

The ratio of the absorption found by selecting the brightest objects to the true average absorption has been calculated on the basis of the cloud model for the absorbing material which is described in Appendix 3. The model is based upon the hypothesis that all of the absorbing material is in the form of interstellar clouds which are Poisson-distributed along the line of sight. The ratio of the "observed"

to true absorption is then independent of cscb, and depends only upon one parameter, the optical depth of the typical cloud.

With the parameters of a "standard cloud" given by Spitzer (1968), we find 0.2 magnitude for the absorption produced by one cloud, and 0.76 for the ratio of "observed" to true absorption.

Thus, the galaxy counts in the annulus around each cluster and the cloud model for the absorbing material confirm the estimate of 0.75 as the amount by which the equal weight solution underestimates the absorption and reddening.

IV. CONCLUSION

The two cases for the distribution of the absorbing material which were considered in the previous section may be regarded as bounding the true case. Taking an average of the values found in the two cases as being most representative of the true situation, the ratio of total to selective absorption is found to be $A_V/E_{V-r}=3.9$. Here, the polar absorption in the V band is $A_V=0.06$, and the polar color-excess is $E_{V-r}=0.016$. However, with only this small sample of 55 objects available, the absorption and reddening could have been underestimated.

Using Whitford's (1958) curve for absorption as a function of wavelength, R=3.6 for the V and r band passes. This value is bounded by 3.4 and 4.4, the values of R for the two cases, and may be considered to be in good agreement with R=3.9, found above.

Again using Whitford's curve, we find that the absorption in the blue or photographic band pass is approximately 1.3 times the absorption in the V band pass. Thus, the expected absorption and reddening for the B and V pass bands is $A_B=0.08$ and $E_{B-V}=0.02$.

These findings are in agreement with those of Sandage (1964a, 1964b) and Sturch (1966) for the color-excess at the galactic pole, but they are in conflict with the large value for the absorption ($A_{pg}=0.5$) derived from the galaxy counts.

Holmberg (1968) has suggested that the increasing number of faint stars at decreasing galactic lattitude may have caused more galaxies to be missed at lower latitudes. This would cause the absorption indicated by the galaxy counts to be an overestimate of the true situation.

Clearly, more work is required in order to resolve the conflict between the large value for the absorption indicated by the galaxy counts and the low values for the reddening and the ratio of total to selective absorption.

A1 - A SEQUENCE OF UBVr STANDARD STARS FOR LARGE TELESCOPES

Introduction

The observations of the galaxies were reduced to colors and magnitudes outside the atmosphere with the assistance of a standard sequence of stars which were observed each night and which were used to determine the instrumental zero points and the atmospheric extinction. The standard stars were chosen from the Selected Areas on the basis of magnitude and spectral type. They are spaced approximately two hours apart in right ascension at a declination of approximately +30° and are therefore accessible at all seasons with the Newtonian cage in either the north or south position.

The UBVr colors of the standard stars were determined from observations made on the Mt. Palomar 20" telescope of the standard stars and of the primary and secondary standards which define the UBVr system as described by Sandage and Smith (1963). The ubvr (natural) colors of the standard stars were determined from the observations made on the Mt. Wilson 60" and 100" telescopes. The natural and UBVr colors thus determined were used to construct a transformation which relates the natural colors to the UBVr colors, and the inverse transformation, which relates the UBVr colors to the natural colors.

Table A1.1

STANDARD STARS

BD	α (1950)	δ (1950)	Sp	V	V-r	B-V	U-B	n
30.50	00 20 42	31 03 42	d:K0	10.19	0.91	1.25	1.11	11
28.426	02 27 31	29 21 52	B9	10.56	0.03	0.03	-0.24	10
30.663	04 22 40	30 15 52	A0	10.27	0.39	0.53	0.27	7
30.1243	06 26 14	30 47 11	F3	10.64	0.39	0.47	0.08	7
30.1705	08 21 24	30 16 41	d::G0	9.93	0.56	0.73	0.30	8
30.2020	10 26 02	30 22 07	K2	10.08	0.80	1.13	0.99	8
29.2232	11 53 29	29 23 31	A5	10.60	0.16	0.24	0.06	7
30.2470	13 55 22	29 58 51	F5	10.48	0.39	0.50	0.00	10
30.2726	15 55 17	29 55 05	dG8	10.08	0.66	0.93	0.65	9
30.3075	17 50 41	30 07 28	g::K3	9.97	0.98	1.38	1.33	10
28.3590	20 00 12	28 31 28	B9	10.12	0.09	0.14	-0.12	10
30.4565	21 54 59	30 50 15	dG5	10.28	0.51	0.68	0.24	16

n - number of observations
Sp - from Bergedorfer Spectral Durchmusterung

Determination of the UBVr Colors for the Standard Stars

The determination of the UBVr colors for the standard stars was done in two basic steps: first, the extinction was determined so that colors and magnitudes could be reduced to outside the atmosphere; second, the colors and magnitude on the natural system reduced to outside the atmosphere were compared with the UBVr colors for the same stars, and a transformation relating the UBVr system to the natural system was deduced. The inverse transformation was then used to convert the natural colors of the unknowns to UBVr colors.

It was assumed that the effects of atmospheric extinction upon the colors could be adequately described by the following equations:

$$\begin{aligned} v &= v_o + K_v \cdot X + Z_v \\ (v-r) &= (v-r)_o + K_{v-r} X + Z_{v-r} \\ (b-v) &= (b-v)_o + K_{b-v} X + Z_{b-v} \\ (u-b) &= (u-b)_o + K_{u-b} X + Z_{u-b} . \end{aligned} \tag{A1.1}$$

Here the subscript o refers to the color outside the atmosphere, and X is the air mass computed from a polynomial approximation (Hardie, 1962) to Bemporad's values.

$$\begin{aligned} X = \sec\mu &- 0.0018167(\sec\mu - 1) \\ &- 0.002875(\sec\mu - 1)^2 - 0.0008083(\sec\mu - 1)^3 \end{aligned} \tag{A1.2}$$

$$\sec\mu = (\sin\varphi \sin\delta + \cos\varphi \cos\delta \cos h)^{-1} \qquad \text{(A1.3)}$$

φ is the observer's latitude, and δ and h are the declination and hour angle of the object observed.

In equation (A1.1) Z is taken to be constant throughout any given night and K was assumed to have the form:

(A1.4)

$$\begin{aligned} K_v &= K'_v + K''_v \cdot (b-v) \\ K_{v-r} &= K'_{v-r} + K''_{v-r} \cdot (v-r) \\ K_{b-v} &= K'_{b-v} + K''_{b-v} \cdot (b-v) \\ K_{u-b} &= K'_{u-b} + K''_{u-b} \cdot (u-b). \end{aligned}$$

K' was allowed to be time-dependent, but in practice any night which could not adequately be reduced with a constant K' was thrown out.

Figure A1.1 illustrates the linear relation between the observed v (plotted with the addition of an arbitrary constant, different for each star) and airmass that was assumed in equation (A1.1). The line in Figure A1.1 corresponds to equation (A1.2) with $K_V = 0.160$.

The observations made on November 24 and 25, 1967, were taken to define the natural system for the Palomar 20" telescope. Equation (A1.1) was solved separately for each star with Z = 0, using the observations made on November 24 and 25. With the natural colors outside the atmosphere

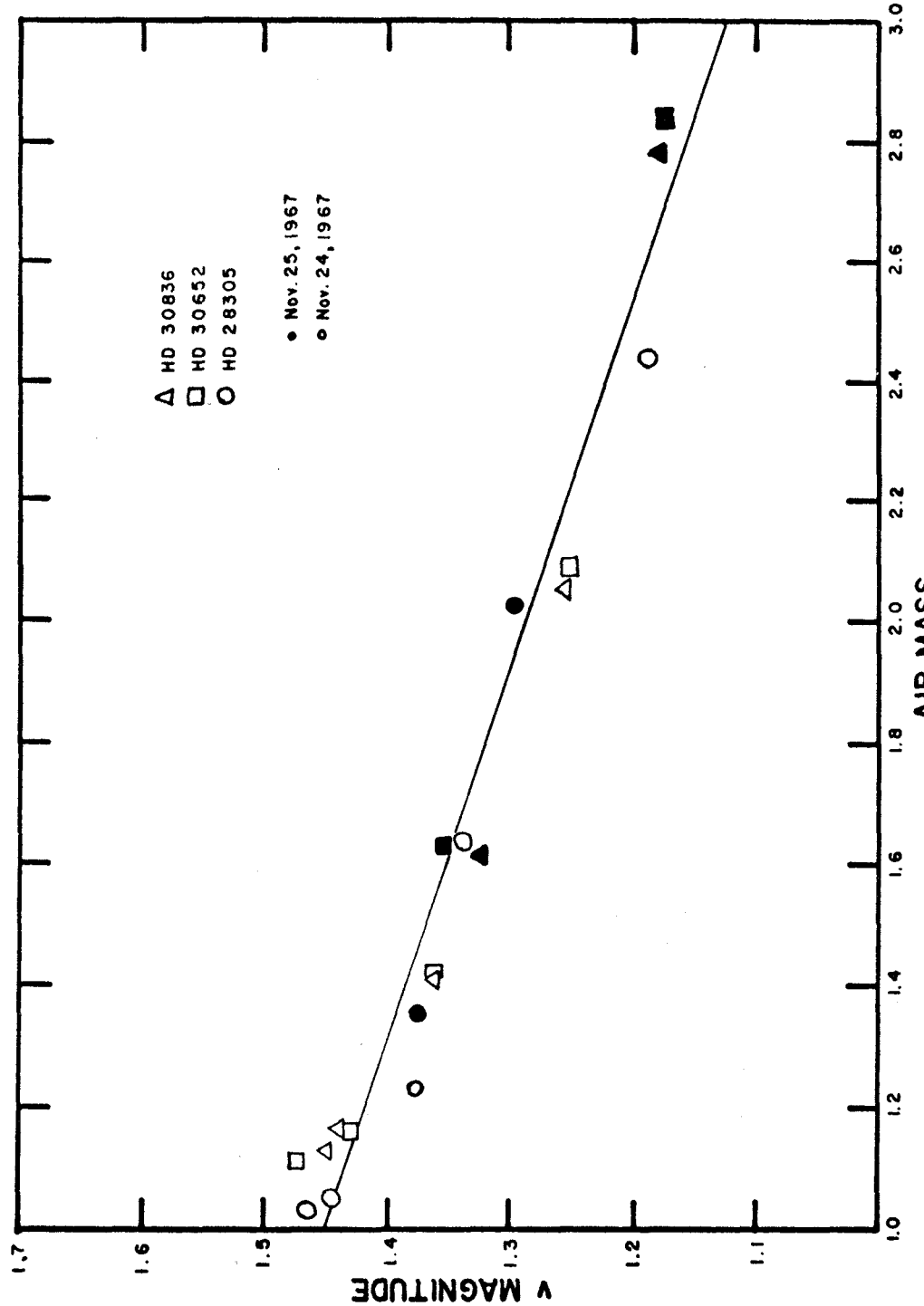

A1.1 v magnitude (plus constant) for three stars of different colors vs. air mass.

obtained from the solution above, K was calculated for each observation using equation (A1.1) with Z = 0.

Figure A1.2 illustrates the linear relation between the extinction K_{b-v} (calculated as above) and the observed (b-v) that was assumed in equation (A1.4). The line in figure A1.2 corresponds to equation (A1.4) with $K'_{b-v} = 0.115$ and $K''_{b-v} = 0.033$.

The values for the extinction coefficients for November 24 and 25, 1967 are given in Table A1.2.

TABLE A1.2

	v	v-r	b-v	u-b
K'	0.164	0.075	0.115	0.245
K''	-0.005	-0.040	-0.033	-0.027

All the observations made on these two nights were then reduced, using the values for the extinction coefficients given in Table A1.2.

The natural colors outside the atmosphere obtained above were now related to the UBVr colors through a system transformation which had the following form:

$$M_i^S = \sum_{j=1}^{j=4} S_{ij} M_j^N + Z_i \qquad \text{(A1.5)}$$

The inverse transformation is:

$$M_i^N = \sum_{j=1}^{j=4} S_{ij}^{-1} (M_j^S - Z_j) \qquad \text{(A1.6)}$$

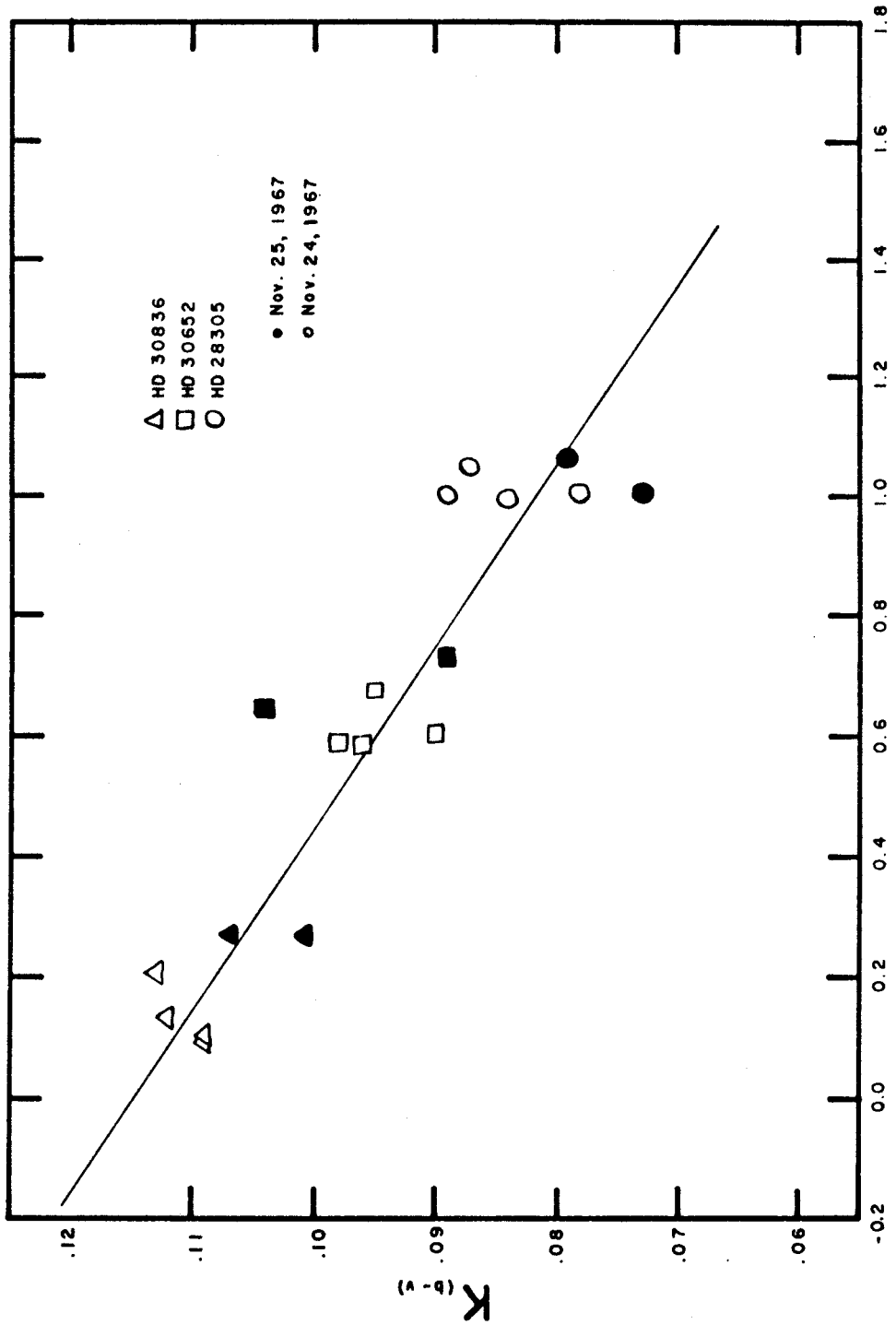

A1.2 Extinction coefficient vs. observed color for three stars

Here i,j run from 1 to 4 denoting v, v-r, b-v, and u-b, while the superscripts N and S denote the natural ubvr system and the standard UBVr system, respectively.

Figure A1.3 illustrates the linearity of the transformation equations (A1.5) and (A1.6). It was found that for the colors, S could be taken to be diagonal since the colors were correlated only with themselves. That is, the residuals from the linear relation illustrated in Figure A1.3 were not correlated with v-r, thus indicating that no correction for a red leak was required. However, a color term was included in the transformation to correct for the color dependence of v illustrated in Figure A1.4. The elements of the transformation matrix S, and the zero points $\mathcal{Z}$ which were derived from 28 observations of 13 UBVr standards on the nights of November 24 and 25, are given below.

$$S = \begin{matrix} 1.000 & 0.0 & -0.068 & 0.0 \\ 0.0 & 1.100 & 0.0 & 0.0 \\ 0.0 & 0.0 & 1.279 & 0.0 \\ 0.0 & 0.0 & 0.0 & 1.122 \end{matrix}$$

$$\mathcal{Z} = \begin{matrix} 0.048 & -0.134 & -0.143 & 0.268 \end{matrix}$$

With the system transformation in hand, the observations made with the Palomar 20" telescope in May and August of 1967 were reduced as follows: The extinction coefficients were calculated from the observed natural colors of the standards and the natural colors outside the atmosphere,

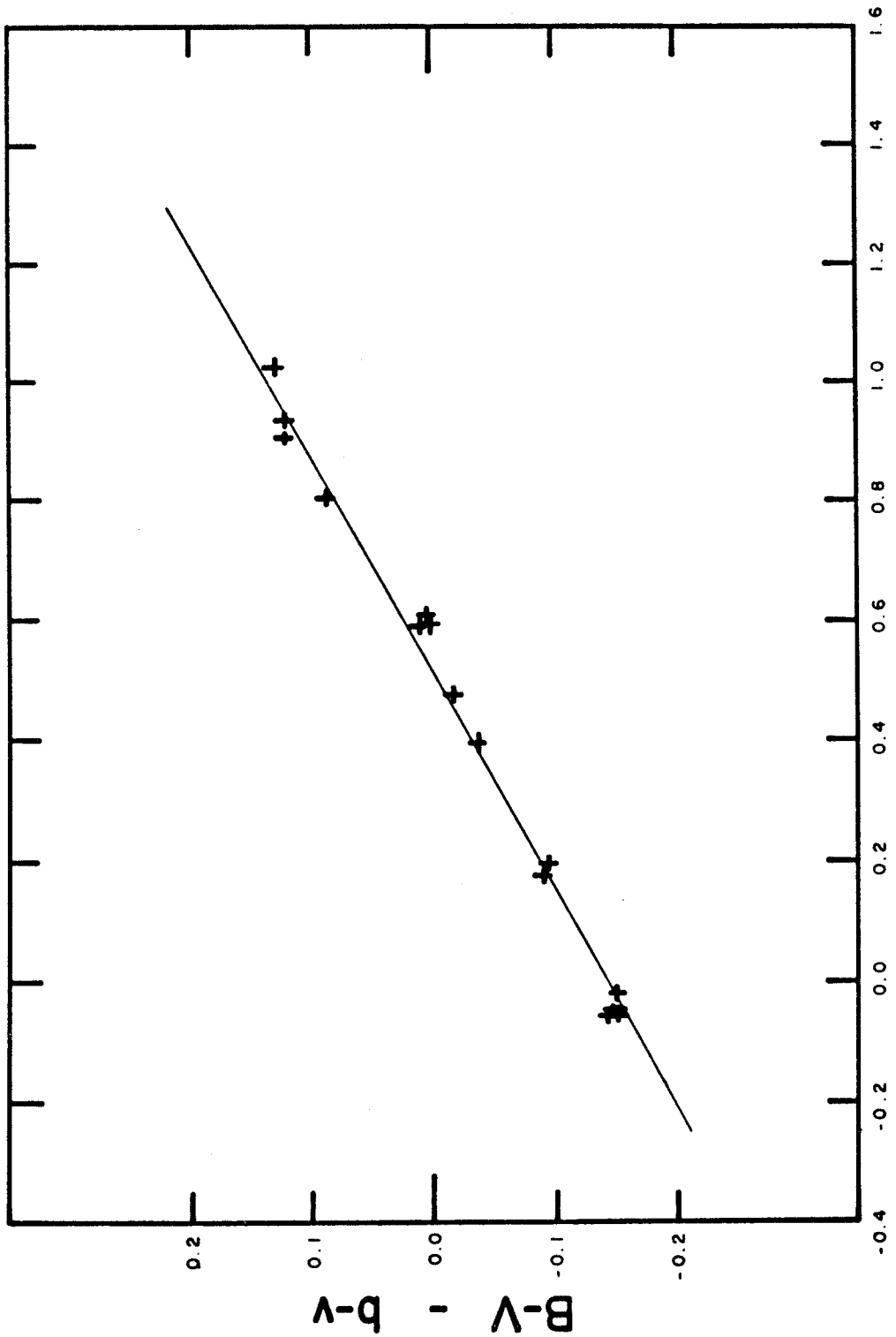

A1.3 Standard minus natural colors vs. natural colors

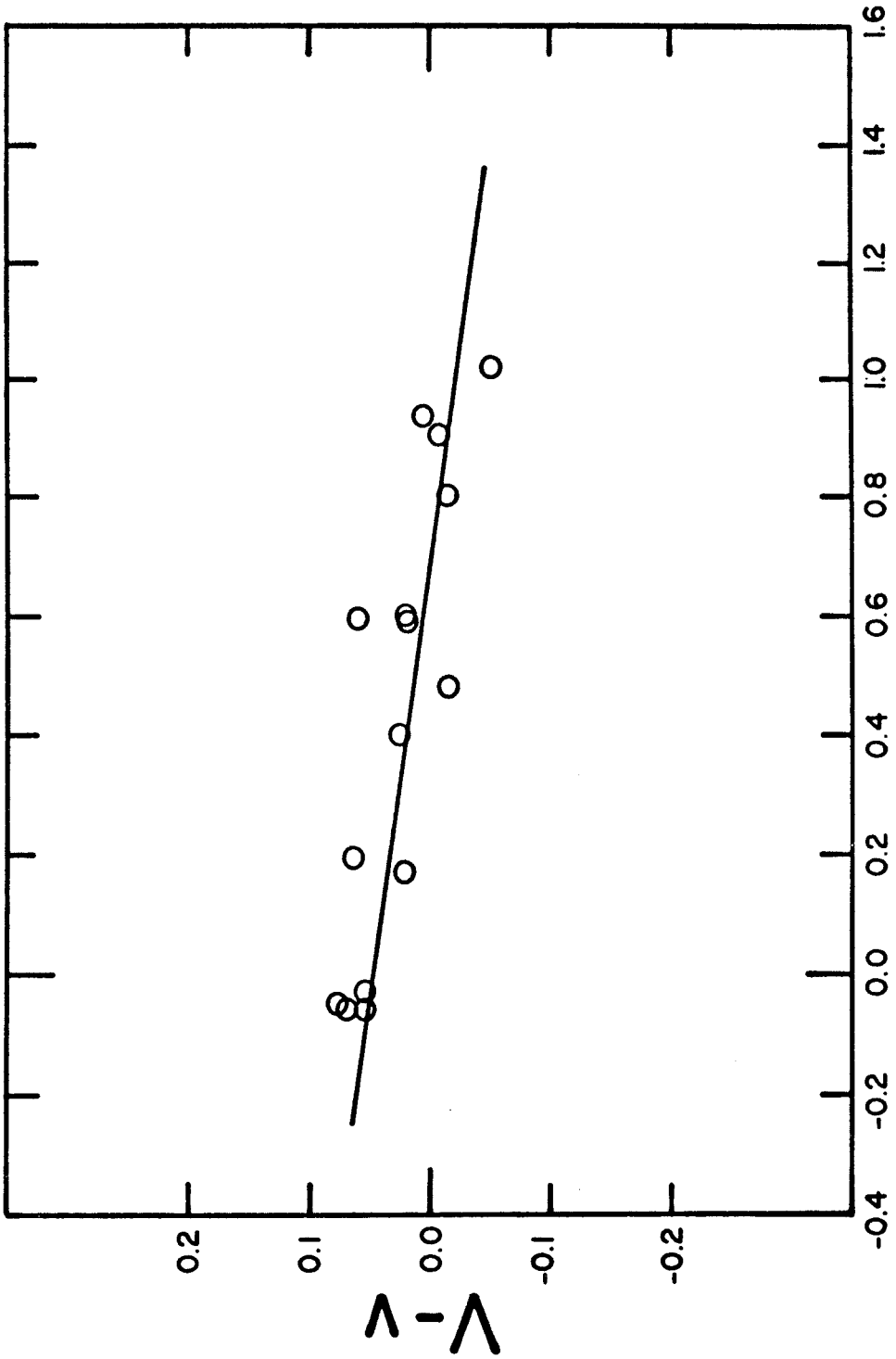

A1.4 Standard minus natural magnitudes vs. natural colors.

which were obtained by transforming the colors of the UBVr standards to the natural system. All the unknowns were then reduced to natural colors outside the atmosphere, and the inverse system transformation was applied to obtain the UBVr colors of the unknowns. It was assumed that, while K' and Z varied from night to night, K" and the system transformation S and Z would remain constant.

The UBVr colors derived for the standard stars and listed in Table A1.1 are the result of eight nights of observations in May, August, and November of 1967. Each standard star was observed an average of ten times and on an average of four different nights.

The average error in the colors given in Table A1.1 for the standard stars should be less then $\pm 0.^{m}02$. Figure A1.5 shows the errors in the observations of the V magnitudes of the UBV standards which were observed on these same nights to determine the extinction. δV is the difference between the V magnitude given by Johnson and Morgan (1953) and the observed V magnitude after it was corrected for the extinction and transformed from the natural system. Similarly, $\delta(V-r)$ is the difference between the V-r color given by Sandage and Smith (1963) and the observed V-r color after correction for the atmospheric extinction and the natural system.

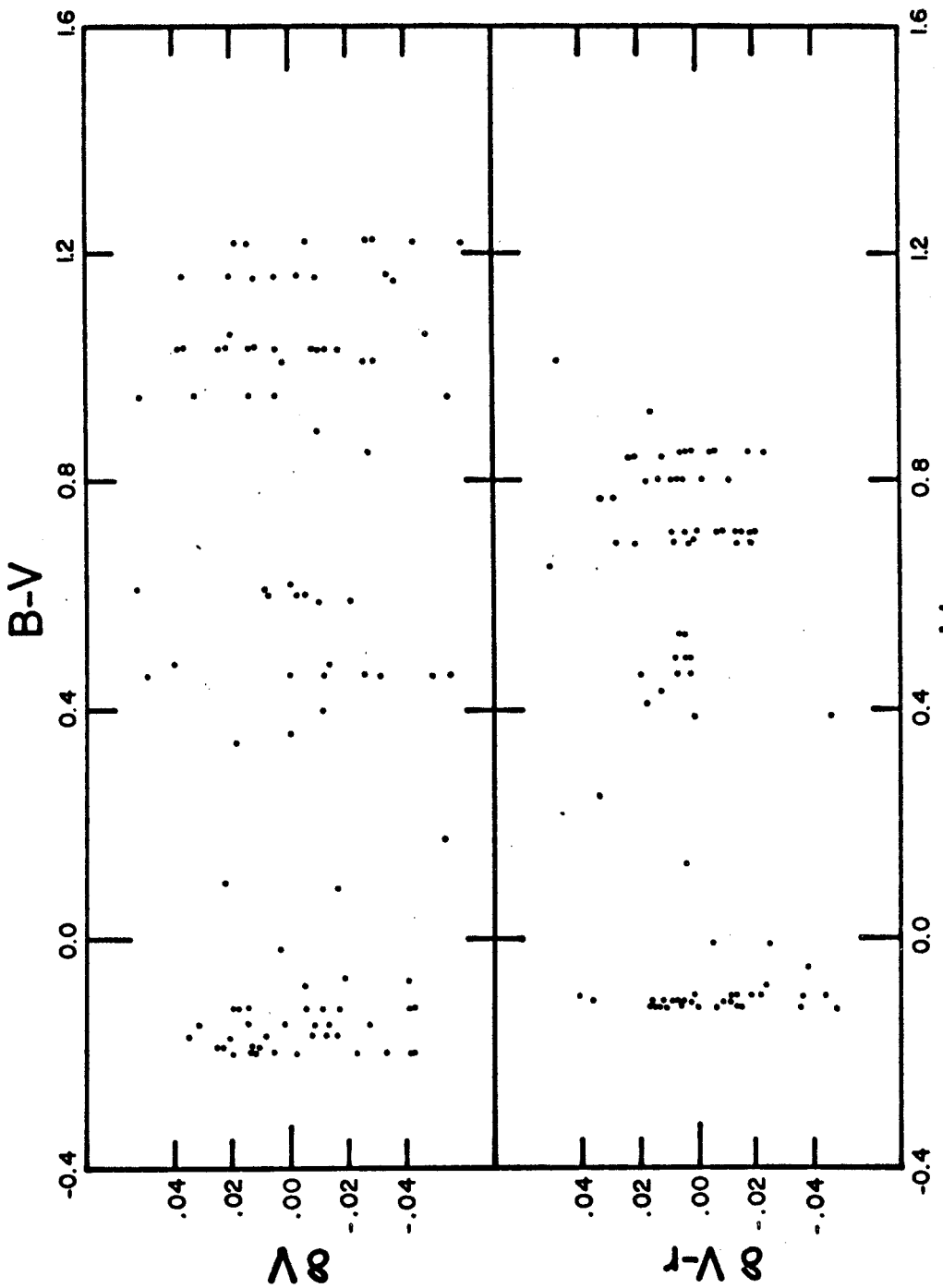

A1.5 Residuals of V and V-r vs. B-V and V-r.

Mt. Wilson Observations with the Standard Stars

On a typical night, three to six of the standard stars would be observed at the beginning, middle, and end of the night. Since no single star was usually observed more than twice on the same night, and since all the standard stars could not be observed on any one night, the Mt. Wilson natural system was determined by solving simultaneously for the extinction coefficient and the zero offset for each night as well as for the natural colors of each star outside the atmosphere. In this way, all the observations taken for this program are locked together by the same set of standards, and the systematic errors caused by observing different standards in different seasons are minimized.

The solution proceeds as follows. Let Y be a column vector computed from the observations, so that:

$$Y^{\alpha}_{ijn} = C^{\alpha}_{ijn} - C^{\beta}_{ijn} K''_{\alpha} X_{ijn} \qquad \text{(A1.7)}$$

Here C^{α} denotes a color v, v-r, b-v, or u-b, and C^{β} denotes the color used in computing the second-order extinction so that when $C^{\alpha} = v$, $C^{\beta} = b-v$ and for all other values of C^{α}, $C^{\beta} = C^{\alpha}$ as in equation (A1.4). The index i denotes the standard star that was observed, and the index n denotes the night on which the observation was made.

The index j numbers the observations of star i that were made on night n. Thus, X_{ijn} is the airmass for the jth observation of the ith standard which was observed on night n. The values of K"α which were used are given in Table A1.2.

Using equations (A1.1) and (A1.4) we see that Y^{α}_{ijn} as defined in equation (A1.7) is simply

$$Y^{\alpha}_{ijn} = C^{\alpha}_{oi}\,\delta^{\mu}_{i} + K'^{\alpha}_{n}\,X_{ijn}\,\delta^{\nu}_{n} + Z^{\alpha}_{n}\,\delta^{\nu}_{n} \qquad \text{(A1.8)}$$

where μ is an index over the standard stars and ν is an index over the nights on which the observations were made.

$$\delta^{\mu}_{i} = \begin{cases} 1 & \mu = i \\ 0 & \text{otherwise} \end{cases} \qquad \delta^{\nu}_{n} = \begin{cases} 1 & \nu = n \\ 0 & \text{otherwise} \end{cases} \qquad \text{(A1.9)}$$

Here C^{α}_{oi} is the color outside the atmosphere of standard number i, and K'^{α}_{n} and Z^{α}_{n} are the extinction coefficient and zero offset for the nth night.

Let X^{α}_{A} be a column vector of the form:

$$X^{\alpha}_{A} = \left[C^{\alpha}_{o1}, C^{\alpha}_{o2}, \cdots C^{\alpha}_{oI}, K'^{\alpha}_{1}, K'^{\alpha}_{2}, Z^{\alpha}_{2}, \cdots K'^{\alpha}_{N}, Z^{\alpha}_{N}\right] . \qquad \text{(A1.10)}$$

Let $F_{ijn,A}$ be a matrix computed from the observations so that:

$$F_{ijn,A} = \left[\delta^{1}_{i}, \delta^{2}_{i}, \cdots \delta^{I}_{i}, X_{ijn}\delta^{1}_{n}, X_{ijn}\delta^{2}_{n}, \delta^{2}_{n}, \cdots X_{ijn}\delta^{N}_{n}, \delta^{N}_{n}\right] . \qquad \text{(A1.11)}$$

From the definition (A1.10) and (A1.11) we see that equation (A1.8) can be written as:

$$\sum_{A} F_{ijn,A} \cdot X_{A}^{\alpha} = Y_{ijn}^{\alpha} \quad . \tag{A1.12}$$

We obtain the extinction coefficients and zero offsets as well as the natural colors of each star outside the atmosphere by solving equation (A1.12) for X^{α}.

Clearly from equation (A1.12)

$$\sum_{ijn} F_{B,ijn}^{-1} \sum_{A} F_{ijn,A} X_{A}^{\alpha} = \sum_{ijn} F_{B,ijn}^{-1} Y_{ijn}^{\alpha} \quad . \tag{A1.13}$$

Inverting the order of the sums we have

$$\sum_{A} \sum_{ijn} F_{B,ijn}^{-1} F_{ijn,A} X_{A}^{\alpha} = \sum_{ijn} F_{B,ijn}^{-1} Y_{ijn}^{\alpha} \quad . \tag{A1.14}$$

By definitions:

$$\sum_{ijn} F_{B,ijn}^{-1} F_{ijn,A} = \delta_{B,A} \quad . \tag{A1.15}$$

Thus we have for X^{α}:

$$\sum_{A} \delta_{B,A} X_{A}^{\alpha} = X_{B}^{\alpha} = \sum_{ijn} F_{B,ijn}^{-1} Y_{ijn}^{\alpha} \quad . \tag{A1.16}$$

$F_{B,ijn}^{-1}$ is obtained by numerical computation from $F_{ijn,A}$ which is constructed directly from the observations. Since

the computation of $F^{-1}_{B,ijn}$ required the inversion of a 60x60 matrix, equation (A1.15) was evaluated numerically as a check on the matrix inversion. It was found that the largest off-diagonal element of $\delta_{B,A}$ was less than 10^{-5} and that the diagonal elements differed from unity by even less than this, giving an accuracy two orders of magnitudes better than that of the observations themselves.

In Table A1.3 are the values of K^{α} and Z^{α} found from the evaluation of X^{α} in equation (A1.16). In order that K' and Z be well determined, the observations of all good nights in a particular run were combined, with the assumption that K' and Z were constant over a period of a few days. This assumption was verified by examining each night individually.

As can be seen in the table, the variations in K' may be somewhat seasonal, while the variations in Z are not correlated with season or telescope.

The fact that the zero points for the 60" and 100" telescopes are not systematically different may be taken as an indication that the coincidence corrections are properly applied.

The coincidence corrections were measured in the Pasadena laboratory using the same electronic equipment that was used to make the observations at the telescope. The procedure used was to measure the light transmitted by 5 neutral density filters at 7000A at different light levels. The light levels were adjusted so that the highest counting

TABLE A1.3

Date		K_V	Z_V	K_{V-r}	Z_{V-r}	K_{B-V}	Z_{B-V}	K_{U-B}	Z_{U-B}
Jan. 1967	60"	0.181	0.	0.083	0.	0.091	0.	0.250	0.
Dec. 1966	60"	0.192	-0.082	0.076	-0.007	0.101	-0.017	0.275	-0.016
Feb. 1967	100"	0.144	-0.135	0.066	-0.030	0.113	0.033	0.300	0.040
Mar. 1967	100"	0.205	-0.084	0.083	-0.014	0.094	0.061	0.310	-0.005
Apr. 1967	60"	0.183	0.126	0.081	0.041	0.065	0.105	0.140	0.151
Dec. 1967	60"	0.161	0.213	0.057	0.203	0.014	0.006	0.184	-0.006
Jan. 1968	100"	0.173	0.201	0.068	0.166	0.101	0.105	0.222	0.046

rate of one level was greater than the lowest counting rate of the next level. The ratios of the filters, determined by extrapolating the ratios derived from the measurements described above to zero counting rate, were in good agreement with independent measures made with a high speed laboratory pulse counting system at a low counting rate.

Figure A1.6 shows the coincidence correction as a function of the observed counting rate. Indicated in the figure is the typical counting rate of a standard star at the 100" which represents the highest counting rates encountered in the program.

The Mt. Wilson observations were reduced to natural colors outside the atmosphere using the natural colors, C_o, of the standard stars that were obtained from the solution of equation (A1.16). These are tabulated on page 64.

Using the natural colors outside the atmosphere which are given in Table A1.4 and the UBVr colors in Table A1.1, the system transformation for the Mt. Wilson natural system was deduced.

The elements of the transformation matrix and the system zeros are given below:

$$S = \begin{matrix} 1.0 & 0.122 & 0.0 & 0.0 \\ 0.0 & 0.995 & 0.0 & 0.0 \\ 0.0 & 0.0 & 1.279 & 0.0 \\ 0.0 & 0.0 & 0.0 & 0.835 \end{matrix}$$

$$Z = \begin{matrix} -0.298 & 0.462 & 0.629 & 0.505 \end{matrix}$$

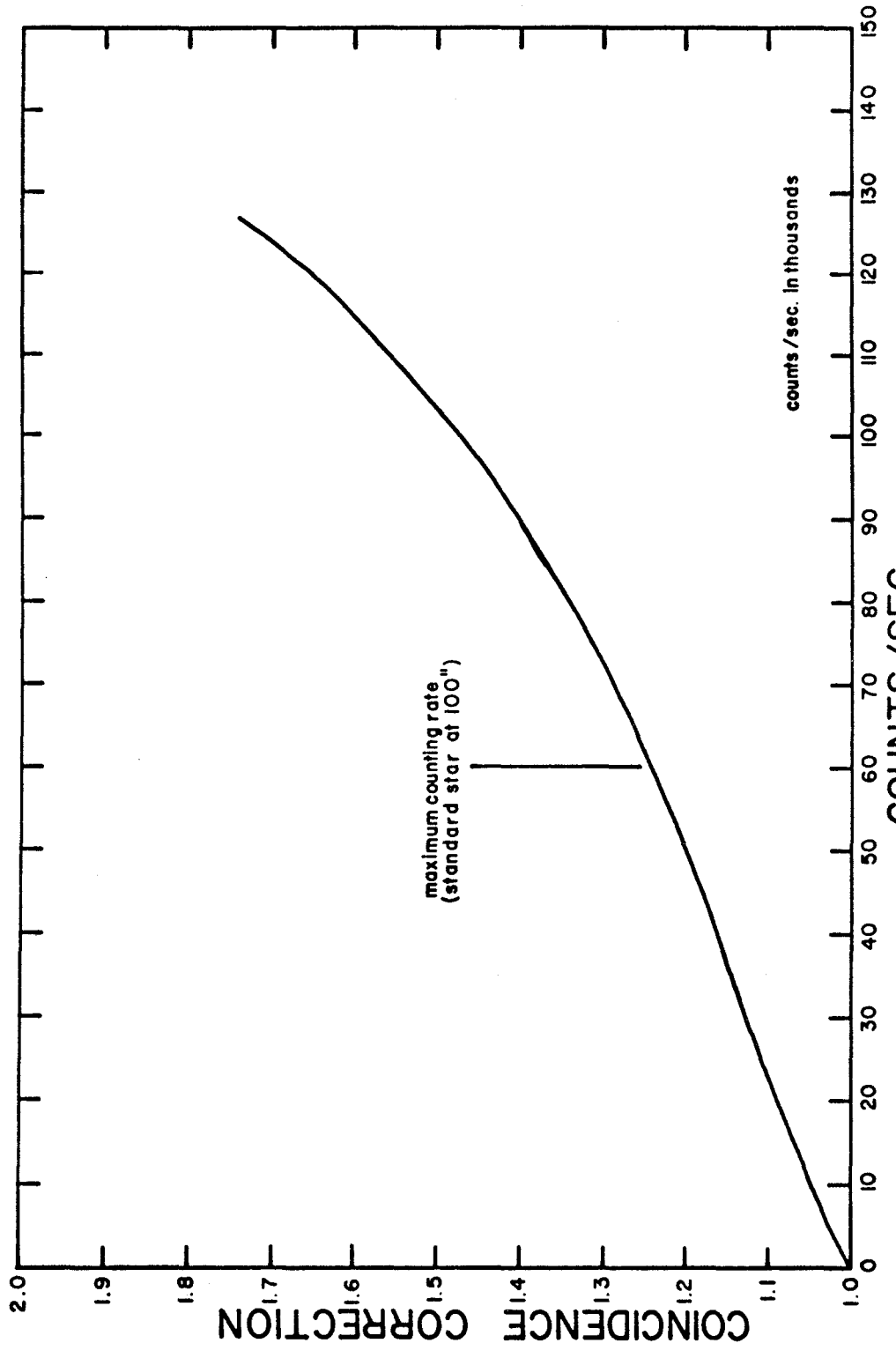

A1.6 Coincidence correction vs. observed counting rate.

TABLE A1.4

BD	v	v-r	b-v	u-b	n
30.50	10.519	0.449	0.493	0.762	8
28.426	10.794	-0.445	-0.472	-0.819	4
30.663	10.556	-0.071	-0.085	-0.249	14
30.1243	10.941	-0.090	-0.118	-0.521	11
30.1705	10.253	0.093	0.076	-0.294	25
30.2020	10.448	0.346	0.392	0.612	11
29.2232	10.863	-0.284	-0.317	-0.553	9
30.2470	10.756	-0.057	-0.097	-0.631	14
30.2726	10.392	0.219	0.229	0.088	7
30.3075	10.324	0.529	-0.581	0.996	2
28.3590	10.374	-0.382	-0.377	-0.711	2
30.4565	10.578	0.052	0.042	0.329	3

n = number of observations.

Figure A1.7 illustrates the dependence of V upon v-r and the linear relation between B-V and b-v.

The observations of the galaxies were transformed from the natural system to the UBVr system using the system transformation equation (A1.5) and the values for S and $\mathcal{Z}$ given above. For V and V-r we have:

$$V = v - 0.122\ (v-r) - 0.298 \qquad \text{(A1.17)}$$

$$V - r = 0.995\ (v-r) + 0.462 \qquad \text{(A1.18)}$$

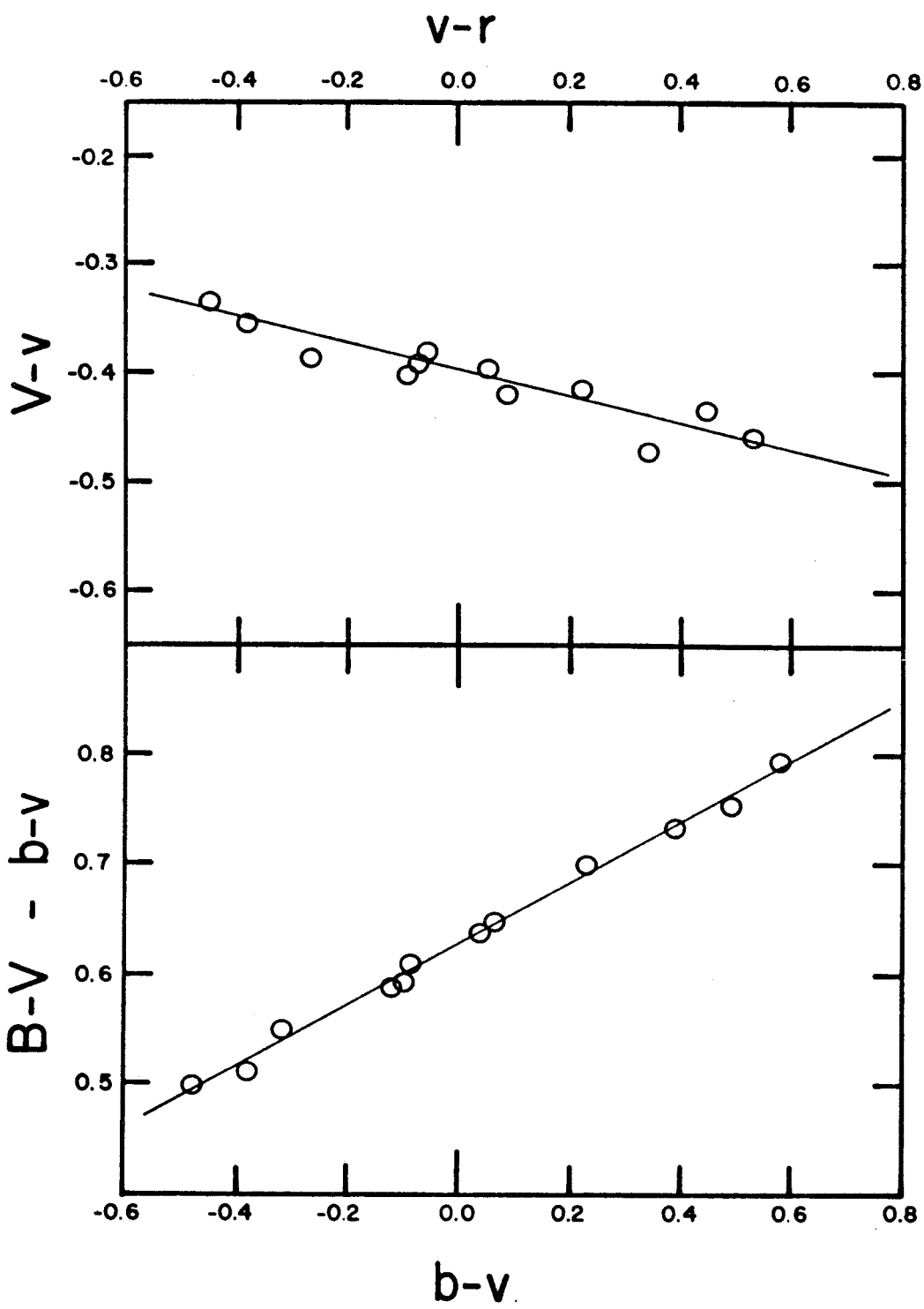

A1.7 Standard minus natural colors and magnitudes vs. natural colors.

A2 - K - CORRECTIONS AND APPARENT DIAMETERS

Cosmological Models

We adopt the postulate that the universe is homogeneous and isotropic. This implies that it has a constant curvature, and that the most general form of the line element can be written as (Robertson, 1929, and Walker, 1936):

$$ds^2 = c^2 d\tau^2 - R^2(\tau)\left(du^2 + \sigma_K^2(u)\, d\gamma^2 \right) \qquad \text{(A2.1)}$$

where $\sigma_K(u)$ takes on the forms:

$$\sigma_K(u) = \begin{cases} \sin u & K = 1 \\ u & K = 0 \\ \sinh u & K = -1 \end{cases} . \qquad \text{(A2.2)}$$

We define

$$H \equiv \frac{\dot{R}}{R} \qquad \text{(A2.3)}$$

and

$$q \equiv - \frac{\ddot{R}}{R H^2} \qquad \text{(A2.4)}$$

where

$$\dot{} = \frac{d}{d\tau} .$$

We note that the redshift z, which is defined in terms of the ratio of the wavelength observed, λ_o, to the wavelength emitted, λ_e, is also equal to the ratio of the curvature parameter at the time of observation, $R(\tau_o)$, to the curvature parameter at the time of emission, $R(\tau_e)$. (McVittie, 1964).

$$1+z = \frac{\lambda_o}{\lambda_e} = \frac{R(\tau_o)}{R(\tau_e)} \qquad \text{(A2.5)}$$

We shall consider only the solutions of the Einstein field equations without rotation, shear and cosmological constant. Neglecting the effects of pressure and radiation at the present epoch, we shall attribute the gravitational field to the matter density alone.

We then have (Mattig, 1958)

$$R_o\tau(u) = \begin{cases} \frac{c}{H_o}\left[z(1+z)\right]/(1+z) & q_o = 0 \\ \frac{c}{H_o}\left[\frac{1}{q_o^2}\left(q_o z + (q_o - 1)\right)\left(\sqrt{1+2q_o z} - 1\right)\right]/(1+z) & \end{cases} \qquad \text{(A2.6)}$$

where $R_o = R(\tau_o)$, $H_o = H(\tau_o)$, and $q_o = q(\tau_o)$

Metric Diameters

Consider two photons originating at opposite points of a galaxy (du = o) which are observed at the same instant ($d\tau = o$) by an observer. We see from the metric (A 2.1) that the distance (ds) separating the two points is:

$$y = R(\tau_e)\, S_k(u)\, \theta \quad . \tag{A2.7}$$

Here, $d\gamma = \theta$, is the angular separation of the points as seen by the observer. Using equation (A2.5) and equation (A2.7) we have:

$$\theta = \frac{y(1+z)}{R_o S_k(u)} \tag{A2.8}$$

where $R_o S_k(u)$ is given by equation (A2.6) as a function of the redshift, z.

K - Corrections

When measurements are made of the radiant flux received from a source which is moving with a velocity with respect to the observer, corrections must be made to the measured flux to correct for the effects resulting from the relative motion. These effects are threefold. The band pass of the detector in the observers frame, which has an effective wavelength λ, detects radiation from the source at an

effective wavelength of approximately $\lambda/(1+z)$. The wavelength width of the detector's band pass, in terms of emitted wavelengths, is also less by a factor of $1/(1+z)$. Also, the total flux received in the band pass of the detector is less by a factor of $1/(1+z)^2$ than the flux emitted by the source in the region of its spectrum that is being received by the detector.

The K - correction used in this study is so defined that it corrects the magnitude, derived from a flux measurement using a detector with a given band pass and effective wavelength, to that which would have been measured by the same detector, if there had been no relative velocity between the observer and the emitter. It is identical to that used by Hubble (1936).

Humason, Mayall and Sandage (1956) and Oke and Sandage (1968) have used a K - correction, K_s, which does not include the factor of $1/(1+z)^2$.

Let the absolute magnitude of an object be defined as:

$$M \equiv -2.5 \log \left\{ \frac{\int_0^\infty S(\nu) L_e(\nu) \, d\nu}{4\pi p_s^2} \right\} . \qquad \text{(A2.9)}$$

$S(\nu)$ is the response function of the detector. $L_e(\nu)$ is the luminosity of the object at the frequency ν in ergs/sec per frequency interval. p_s is a standard distance, taken to be 10 parsecs. The quantity in the brackets is, then, the

flux measured by the detector when the object is 10 parsecs distant and at rest with respect to the detector.

The monochromatic flux in the observer's frame $F_o(\nu)d\nu$ is related to the flux in the emitter's frame, $F_e(\nu_e)d\nu_e$ by

$$F_o(\nu)d\nu = \frac{F_e(\nu_e)d\nu_e}{(1+z)^2} \qquad \text{(A2.10)}$$

This may be seen by Lorentz transforming the Poynting vector. A detector with a response function $S(\nu)$ will measure a flux, f (0), when moving with the emitter, and a flux, f (z), when the emitter has a redshift z.

$$f(0) = \int_0^\infty S(\nu) F_e(\nu) d\nu \qquad \text{(A2.11)}$$

$$f(z) = \int_0^\infty S(\nu) F_o(\nu) d\nu \qquad \text{(A2.12)}$$

Using the relation $(1+z)\nu = \nu_e$ and equation (A2.12) we have

$$f(z) = \int_0^\infty S(\nu) \frac{F_e(\nu_e)d\nu_e}{(1+z)^2} \qquad \text{(A2.13)}$$

$$= \int_0^\infty S(\nu) \frac{F_e[\nu(1+z)]d\nu}{1+z} .$$

Now if we define:

$$m_o = -2.5 \log f(o) \tag{A2.14}$$

$$m_z = -2.5 \log f(z) \tag{A2.15}$$

$$K(z) = 2.5 \log \left\{ f(o) / f(e) \right\} \quad . \tag{A2.16}$$

we may write:

$$m_o = m_z - K(z) \tag{A2.17}$$

and

$$K(z) = 2.5 \log (1+z) + 2.5 \log \left\{ \frac{\int_o^\infty S(\nu) F_e(\nu) d\nu}{\int_o^\infty S(\nu) F_e[\nu(1+z)] d\nu} \right\} . \tag{A2.18}$$

This is the K - correction defined by Hubble (1936) and is related to the K - correction of Oke and Sandage (1968) by

$$K(z) = K_s(z) + 5 \log (1+z) \quad . \tag{A2.19}$$

We may now relate the flux to the intrinsic luminosity $L_e(\nu)$ of the emitter, by noting that, for an observer traveling with the emitter,

$$F_e(\nu) = \frac{L_e(\nu)}{4\pi R_0^2 \sigma_K^2(w)} \qquad \text{(A2.20)}$$

where $4\pi R_0^2 \sigma_K^2(w)$ is the area of a spherical shell defined by the photons emitted by a source at a metric distance u, which reach the observer at τ_0. $(R_0 = R(\tau_0))$

With equations (A2.13) and (A2.15) we may write:

$$m_z = -2.5 \log \left\{ \frac{\int_0^\infty S(\nu) F_e[\nu(1+z)]\, d\nu}{1+z} \right\} . \qquad \text{(A2.21)}$$

Using (A2.20) this becomes:

$$m_z = -2.5 \log \left\{ \frac{\int_0^\infty S(\nu) L_e[\nu(1+z)]\, d\nu}{(1+z)\ 4\pi R_0^2 \sigma_K^2(w)} \right\} . \qquad \text{(A2.22)}$$

This may be simplified with equations (A2.9) and (A2.18) to:

$$m_z = M + 5 \log R_0 \sigma_K(w) - 5 + K(z) . \qquad \text{(A2.23)}$$

This has the familiar form of:

$$m = M + 5 \log p - 5 + K \qquad \text{(A2.24)}$$

Note that all of the dependence on the cosmological model is contained in $p = R_0 \sqrt{k}(w)$.

For the colors we have:

$$\begin{aligned} V-r &= (V_z - K_V(z)) - (r_z - K_r(z)) \\ &= (V_z - r_z) - (K_V(z) - K_r(z)) \\ &= (V-r)_z - K_{V-r}(z) \,. \end{aligned} \tag{A2.25}$$

A3 - CLOUD MODEL

Let us assume that the absorption takes place in the galactic plane, and that the density of the absorbing material depends only upon the height above the plane. Furthermore, let us assume that the absorbing material occurs in clouds which have a characteristic absorption a_c.

Define $P_b(i)$ as the probability of finding i clouds in the line of sight at latitude b.

Define N(m) as the number of objects with apparent magnitude m in the absence of absorption. Thus, N(m) is the distribution of m outside the galactic plane.

The number of objects which can be observed at magnitude m after suffering an absorption of amount a is N(m-a). Thus, $N(m-a_c i)\ P_b(i)$ is the number of objects at latitude b with magnitude m after suffering an absorption $a = a_c i$. The total number of objects at latitude b with magnitude m is:

$$n_b(m) = \sum_{i=0}^{i=\infty} N(m - a_c i)\, P_b(i) . \qquad \text{(A3.1)}$$

The probability that an object at latitude b with magnitude m has also suffered an absorption a is the fraction of all objects at latitude b with magnitude m that have been absorbed by an amount a.

$$P_b(a|m) = \frac{N(m - a_c i)\, P_b(i)}{\sum_j N(m - a_c j)\, P_b(j)} \qquad a = a_c i \tag{A3.2}$$

The average absorption suffered by objects with apparent magnitude m at latitude b is:

$$\begin{aligned} A_b(m) &= \sum_i p(a_c i \,|\, m) \cdot i a_c \\ &= \sum_a p(a|m)\, a \ . \end{aligned} \tag{A3.3}$$

In selecting the brightest objects, all those with apparent magnitudes less than some limiting apparent magnitude, m_L, were chosen. The average apparent absorption obtained at latitude b is the weighted average of the apparent absorption for each magnitude m:

$$\bar{A}_b = \frac{\int_{-\infty}^{m_L} n_b(m)\, A_b(m)\, dm}{\int_{-\infty}^{m_L} n_b(m)\, dm} \ . \tag{A3.4}$$

To calculate the average true absorption, consider the probability that an object at latitude b has suffered an absorption a. With $a = a_c i$, this is by definition $P_b(i)$.

$$P_b(a) = P_b(i) \qquad a = a_c i \tag{A3.5}$$

The average true absorption suffered by an object at latitude b is then:

$$\overline{A}_b = \sum_a P_b(a)\, a = \sum_i P_b(i)\, a_c\, i \,. \qquad \text{(A3.6)}$$

Let us now consider the form of $P_b(i)$, assuming that the absorption is done by clouds and that the distribution of clouds depends only upon the height above the galactic plane. In this case, the distribution of material may be taken as being made up of many plane parallel layers having various cloud densities. Since the average absorption produced by one layer is proportional to cscb, the average absorption produced by a sum of such layers will also be proportional to cscb.

We shall also assume that the distribution of clouds is independent in that the presence of one cloud does not affect the probability of any others being present. In this case, the probability of having i clouds along the line of sight is given by:

$$P_b(i) = \frac{\nu_b^{\,i}\, e^{-\nu_b}}{i!} \qquad \text{(A3.7)}$$

where:

$$\nu_b = \frac{A \csc b}{a_c} \qquad \text{(A3.8)}$$

Using equation (A3.6) for the true average absorption, and equations (A3.7) and (A3.8), we see that A is the true average absorption at the galactic pole:

$$\overline{A_b} = \sum_i P_b(i)\, a_c i = a_c \nu_b \qquad (A3.9)$$
$$= A \csc b .$$

Let us now consider the form of N(m), assuming that the objects are uniformly distributed in space with some density ρ. Then N(m)dm is the number of objects in a shell whose radius corresponds to m and whose thickness, dr, is related to dm. We will neglect the effects of redshifts here. Then we have:

$$N(m)\, dm = 4\pi \rho R^2 dR . \qquad (A3.10)$$

The relation between m and R is:

$$m = M + 5 \log R - 5 . \qquad (A3.11)$$

Thus:

$$R = 10^{0.2m} \cdot 10^{0.2(5-M)} = K\, 10^{0.2m}$$

$$dR = K \cdot 10^{0.2m} \ln 10\, dm . \qquad (A3.12)$$

N(m) is then:

$$\begin{aligned} N(m)\,dm &= 4\pi\rho R^2 dR \\ &= 4\pi\rho K^3 10^{0.6m}\, dm \\ &= N_0 10^{0.6m}\, dm . \end{aligned} \qquad \text{(A3.13)}$$

With $P_b(i)$ given by equation (A3.7) and N(m) given by (A3.13), the average absorption suffered by objects with apparent magnitude m at latitude b is calculated using equations (A3.2) and (A3.3):

$$A_b(m) = \sum_i p(i a_c | m) \cdot i a_c$$

$$= \frac{\sum_i N(m - a_c i) P_b(i)\, i a_c}{\sum_j N(m - a_c j) P_b(j)} \qquad \text{(A3.14)}$$

$$= \frac{\sum_i N_0 10^{0.6(m - a_c i)} P_b(i)\, i a_c}{\sum_j N_0 10^{0.6(m - a_c j)} P_b(j)}$$

$$= \frac{\sum_i 10^{-0.6 a_c i} P_b(i)\, i a_c}{\sum_j 10^{-0.6 a_c i} P_b(j)}$$

At this point, $A_b(m)$, the apparent absorption of objects with apparent magnitude m is independent of m. Thus, the average apparent absorption at latitude b, $\bar{A}_b$, given by equation (A3.4) becomes $\bar{A}_b = A_b(m)$. Using equation (A3.14) for $A_b(m)$ we have:

$$\bar{A}_b = \frac{\sum_i 10^{0.6 a_c i} P_b(i)\, i\, a_c}{\sum_j 10^{0.6 a_c j} P_b(j)}$$

$$= \frac{\sum_i 10^{0.6 a_c i} \frac{\nu_b^i e^{-\nu_b}}{i!}\, i\, a_c}{\sum_j 10^{-0.6 a_c j} \frac{\nu_b^j e^{-\nu_b}}{j!}} \qquad \text{(A3.15)}$$

$$= a_c \nu_b 10^{-0.6 a_c}$$

$$= A\, 10^{-0.6 a_c \csc b} .$$

Comparing equation (A3.15) with equation (A3.9), we see that the average apparent absorption obtained at any latitude, for any magnitude, will be an underestimate of the true average absorption by $10^{-0.6a}c$. Thus, if we were to observe some object, and if we knew the true average absorption in the vicinity of the object but not for the object itself, we should take $10^{-0.6a}c$ times the true average absorption as the absorption suffered by the object.

REFERENCES

Abell, G.O. 1958, Ap.J.Suppl., 3, 211

Allen, C.W. 1963a, Astrophysical Quantities (2nd ed.; London: U. of London Press), p.122

_____. 1963b, ibid., p.104

Arp, H. 1962, Ap.J., 135, 971

Hardie, R.H. 1962, Astronomical Techniques, ed. W.A.Hiltner (Chicago: U. of Chicago Press), p.180

Holmberg, E. 1958, Medd.Lund.Obs., Ser.II, No.136

_____. 1968 (private communication)

Hubble, E. 1934, Ap.J., 79, 8

_____. 1936, ibid., 84, 517

Humason, M.L., Mayall, N.U., and Sandage, A.R. 1956, A.J., 61, 97

Johnson, H.L., and Morgan, W.W. 1953, Ap.J., 117, 313

Kron, G.E., and Mayall, N.U. 1960, A.J., 65, 581

Lasker, B.M. 1966, Pub.A.S.P., 78, 329

Mattig, W. 1958, A.N., 284, 109

McVittie, G.C. 1965, General Relativity and Cosmology (Urbana: U. of Illinois Press), p.148

Neckel, H. 1965, Zs.f.Ap., 62, 180

Oke, J.B., and Sandage, A.R. 1968 (in press)

Oort, J.H. 1938, B.A.N., 8, 233

Robertson, H.P. 1929, Proc.Nat.Acad.Sci., 15, 822

Sandage, A.R. 1964a, "Ann.Rept.Mt.Wilson Obs.," Carnegie Inst. of Wash.Yrbk., 63, 23

_____. 1964b, Obs., 84, 245

Sandage, A.R., and Smith, L.L. 1963, Ap.J., 137, 1057

Shane, C.D., and Wirtanen, C.A. 1967, Pub.Lick.Obs., 22, 1

Spitzer,L.,Jr. 1968, Nebulae and Interstellar Matter, ed. B.M.Middlehurst and L.H.Aller (Chicago: U. of Chicago Press), p.5

Stebbins,J. 1933,Proc.Nat.Acad.Sci.U.S.,19,222

Sturch,C. 1966,Ap.J.,143,774

_____. 1967,ibid.,148,477

Walker,A.G. 1936,Proc.London Math.Soc.,42,90

Whitford,A.E. 1958,A.J.,63,201